

# SlipStream: Adapting Pipelines for Distributed Training of Large DNNs Amid Failures

Swapnil Gandhi  
Stanford University

Mark Zhao  
Stanford University

Athinagoras Skiadopoulos  
Stanford University

Christos Kozyrakis  
Stanford University

## Abstract

Training large Deep Neural Network (DNN) models requires thousands of GPUs for days or weeks at a time. At these scales, failures are frequent and can have a big impact on training throughput. Restoring performance using spare GPU servers becomes increasingly expensive as models grow.

SlipStream is a system for efficient DNN training in the presence of failures, without using spare servers. It exploits the *functional redundancy* inherent in distributed training systems – servers hold the same model parameters across data-parallel groups – as well as the bubbles in the pipeline schedule within each data-parallel group. SlipStream dynamically re-routes the work of a failed server to its data-parallel peers, ensuring continuous training despite multiple failures. However, re-routing work leads to imbalances across pipeline stages that degrades training throughput. SlipStream introduces two optimizations that allow re-routed work to execute *within* bubbles of the original pipeline schedule. First, it decouples the backward pass computation into two phases. Second, it staggers the execution of the optimizer step across pipeline stages. Combined, these optimizations enable schedules that minimize or even eliminate training throughput degradation during failures. We describe a prototype for SlipStream and show that it achieves high training throughput under multiple failures, outperforming recent proposals for fault-tolerant training such as Oobleck and Bamboo by up to 1.46× and 1.64×, respectively.

## 1 Introduction

Deep Neural Networks (DNNs) are consistently achieving milestone results in domains such as natural language processing [53], speech recognition [24], and computer vision [38]. Since the rapid growth of DNNs is a major contributor to recent breakthroughs [69], we are now in a global race to develop increasingly-large foundation models [8, 25]. Both proprietary [1, 9, 73] and open-source [13, 68] models have tens to hundreds of billions of parameters. Training such models requires uninterrupted access to thousands of accelerators (e.g., GPUs) for several weeks [32, 52, 65]. DNN training is essentially a large supercomputing job that relies on hybrid parallelism, which concurrently leverages data, tensor, and pipeline parallelism strategies [78].

As the scale and duration of training increases, so does the likelihood of encountering failures [18, 21, 29, 32, 74, 79]. While scale-out workloads, such as distributed databases and analytics, are designed to work around server failures, this is not yet the case for DNN training. The rigid parallelization of DNN training implies that each failure can set off a domino effect. All resources are forced to idle while a failed node is replaced and the job is re-optimized and re-started on the new hardware configuration. For example, the training of OPT-175B included 178,000 GPU-hours of wasted time due to various malfunctions [39].

Fault tolerance in DNN training involves three issues: *fault detection*, *checkpointing*, and *efficient execution in the presence of faults*. Large-scale training systems implement comprehensive monitoring of the health of hardware and software components, so that faults or stragglers are quickly detected and diagnosed [32]. Recent research has focused on reducing the overhead of periodic checkpoints of the training job state [18, 36, 49]. Efficient execution in the presence of faults has received less attention. A common approach in industry is to maintain a reserve of spare GPU servers that will replace failed servers when needed. While conceptually simple, this approach is expensive at scale. As the frequency of faults increases, so does the number of spares.

The alternative approach is to *continue training with the subset of resources available*. This is similar to how scale-out systems approach resilience to failures [16]. Data parallelism provides one simple implementation as it creates full replicas of the model across groups of GPUs. When one GPU server fails, we take all the servers in its data-parallel group offline and continue training the remaining model replicas. Unfortunately, this approach increases the blast radius of the failure and its impact to performance. When training a 530B GPT model using the hybrid-parallel scheme of Megatron-LM [51], a single node failure would force 280 GPUs to go offline and cause a roughly 11% drop in training throughput.

Two recent projects have exploited *pipeline parallelism* instead. Bamboo [67] relies on redundant computation and executes each pipeline stage on two nodes even in the fault-free case. When a node fails, the alternative nodes for its stages will do the work. Bamboo’s drawback is the drop in fault-free training throughput due to the redundant computations and added memory pressure on each GPU node.

Oobleck [28] avoids overheads in fault-free execution by pre-computing a number of templates for pipeline parallelism that use a different number of nodes. As nodes fail, Oobleck replaces the original pipeline template with one that uses fewer nodes. The performance challenge for Oobleck is balancing work across heterogeneous pipelines as the pipelines with fewer nodes can become stragglers. Both Bamboo and Oobleck require significant re-configuration as nodes fail or rejoin, which can be a challenge as failure rates increase.

In this paper, we introduce *SlipStream*, a novel scheme for resilient training with hybrid-parallel systems. SlipStream enables efficient execution in the presence of failures, without the need for spares and without any impact on model accuracy. Similar to Bamboo and Oobleck, we exploit pipeline parallelism. But unlike these previous proposals that handle failures within a single pipeline, SlipStream utilizes the inherent *functional redundancy across pipelines* in hybrid-parallel training systems. SlipStream re-routes the micro-batches of failed nodes to *peer nodes* that process the same pipeline stage for the model in the other data-parallel groups. Peer nodes store the same model parameters and can handle the extra work without the need for parameter re-shuffling.

If done naively, SlipStream’s *adaptive pipelining* increases training time and memory usage due to the additional work for the peers of failed nodes. SlipStream uses a series of optimizations that exploit unique characteristics of hybrid-parallel training to eliminate all or most of the inefficiencies. SlipStream uses the *bubbles* in the pipeline schedule of peers to execute the additional work at low or no overhead. These bubbles typically appear during the *start-up* and *cool-down* phase of the pipeline schedule, but not during the *steady-state* when most additional work must occur. SlipStream overcomes this challenge by *decoupling back propagation* for micro-batches into two distinct gradient computations, one relative to the input and one relative to the parameters. The two steps are independently scheduled in order to better leverage bubbles in the *cool-down* portion of the pipeline schedule. The selective application of decoupled back propagation exploits the imbalance in memory usage across stages in hybrid-parallel training while avoiding an increase in peak memory pressure. Finally, SlipStream staggers the execution of the optimizer tasks across pipeline stages in order to leverage bubbles from the *start-up* phase of the pipeline schedule for the next training iteration.

We implemented SlipStream on top of the DeepSpeed training framework [60]. The key SlipStream element is the *Planner* that uses dynamic programming (DP) and mixed integer linear programming (MILP) to find the best pipeline schedule in the presence of multiple failures. The *Planner* runs offline and calculates efficient schedules for up to a certain number of failures. These schedules are employed as needed during training. We evaluated SlipStream using DNNs with billions of parameters like GPT-3 [9], using both real-world experiments and simulations of large training

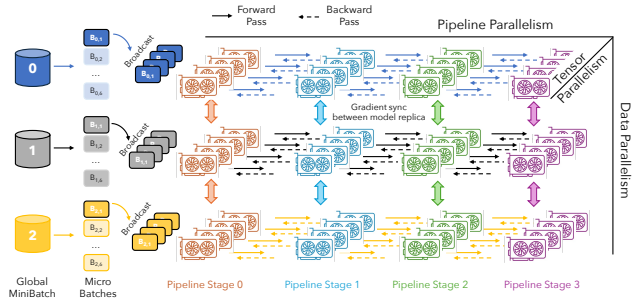


**Figure 1.** Illustration of hybrid parallelism. Pipeline stages are denoted with different colors. Within each pipeline stage, operators are partitioned through tensor parallelism. The global batch is split into micro-batches across pipelines.

systems. We show that SlipStream supports high throughput training even at high failure counts, e.g.  $\geq 10\%$  of the overall system. SlipStream outperforms Oobleck by 1.46 $\times$  in training scenarios with realistic GPU failures. SlipStream’s advantage stems from its efficient scheduling of re-routed work and its ability to avoid major re-shuffling of model parameters upon failures. SlipStream outperforms Bamboo by 1.64 $\times$ . It is also able to efficiently train much larger models than Bamboo, which requires large memory overheads for its fault tolerance mechanism.

## 2 Background and Motivation

### 2.1 Distributed DNN Training

State-of-the-art *Deep Neural Network (DNN)* models consist of tens to hundreds of billions of parameters and are trained on datasets with many trillions of tokens [1, 9, 19, 39, 40, 68, 76]. Their training requires thousands of GPUs for days or weeks [25, 34, 52, 65]. For example, Llama-3 was trained on 15 trillion tokens, using two clusters of 24K GPUs [2].

DNN training is parallelized using three primary forms of parallelism. *Data parallelism (DP)* processes subsets of the input data in parallel across GPU groups, each of which stores the entire model [20, 62, 75]. Data parallelism requires high network bandwidth for the all-reduce operations that reconcile model parameters across all replicas at the end of iteration steps. Tensor and pipeline parallelism are forms of *model parallelism* that facilitate training large models by sharding the model across GPUs. *Tensor parallelism (TP)* partitions the parameters of each layer across GPUs in order to parallelize each linear algebra operation within a layer [64]. It incurs high communication costs that are not easily hidden by computation due to frequent all-reduce operations in both the forward and backward pass. *Pipeline parallelism (PP)* divides the model into sequential groups of layers or *stages*. Micro-batches of data are processed in parallel in a pipelined manner across these stages [26, 35, 42, 45, 50]. Pipeline parallelism requires lower network bandwidth as stages only

communicate activations and gradients at layer boundaries. However, it achieves lower compute utilization as the number of stages increases due to pipeline dependencies and bubbles (idle slots) in the pipeline schedule.

Large-scale training systems balance these tradeoffs by utilizing all three forms of parallelism as shown in Figure 1 [36, 42, 43, 45, 51, 60, 77, 78]. This is known as *hybrid-parallelism*. In the most common case, systems such as DeepSpeed [60] or Alpha [78] use a combination of tensor parallelism within a multi-GPU server, pipeline parallelism across multi-GPU servers, and data parallelism across pipelines. Hybrid parallelism enables large model training with graceful scaling and reasonable training times (weeks to few months) using optimized clusters with 1000s of densely-connected GPUs.

## 2.2 Fault Tolerance in Distributed DNN Training

Large training systems include thousands of GPUs, CPUs, memory chips, networking chips, cables of various types, and power conversion and cooling devices. Scale allows for high performance but also leads to frequent faults ranging from software errors to full hardware malfunctions. The Mean Time Between Failure (MTBF) for large training systems can be minutes [21, 23, 32, 74]. For example, large-scale training clusters at Microsoft see a failure every  $\approx 45$  minutes [29].

In contrast to scale-out frameworks like Map-Reduce [16], which quickly adjust to dynamic changes in resource availability, DNN training operates like a supercomputing job. It relies on fixed sharding and parallelization strategies and gang-scheduled execution. All computational resources must concurrently run uninterrupted, making the system highly susceptible to disruptions from any failure. For example, Meta encountered over 100 hardware failures while training OPT-175B, resulting in the loss of 178,000 GPU-hours [7, 39]. Similar failure rates have been reported by ByteDance [32], Alibaba [23], LAION [6], Microsoft [29] and Google [79]. At this scale, faults are regular occurrences that require systematic optimizations to ensure resilient and efficient training [23, 29, 32, 74].

Enhancing fault tolerance in distributed training involves three key issues: fast error detection, efficient checkpointing, and robust execution under faults. *Fast error detection* is crucial for minimizing downtime and preventing the spread of errors. Some errors can be quickly detected through encoding and redundancy mechanisms in the hardware (e.g., error correction codes) or software timeouts. Other errors are detected if they eventually lead to irregular spikes in the loss function optimized during training [6]. The latter category includes silent data corruptions [4, 14]. *Checkpointing*, which saves the state of the model at regular intervals, allows for recovery from the recent stable state without restarting the entire training from scratch. Since naive checkpointing to remote storage leads to long pauses in the training process, there has been considerable research in improving its efficiency [18, 32, 49, 73] as discussed in Section 6.

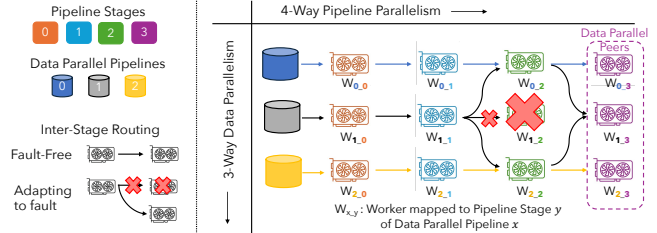


**Figure 2.** Adaptive pipelining when  $W_{1,2}$  fails. The output from worker  $W_{1,1}$  is redirected to workers  $W_{0,2}$  and  $W_{2,2}$ .

## 2.3 Efficient DNN Training in Presence of Failures

Our work focuses on *robust training in the presence of faults*. A common approach is to have a reserve of spares ready to replace servers with failed GPU servers. To reduce recovery time, spare servers can also be *hot standbys* with their memory loaded with model parameters at the end of each iteration. The key advantage of spare servers is that, upon recovery, training efficiency returns to its pre-failure state. However, this approach becomes increasingly costly as systems scale up, fault frequency increases, and more spares are needed. Spare servers must connect to the network of the training cluster with a similar bandwidth profile as the servers they will be called to replace, which incurs additional networking costs and typically requires that spares are allocated in coarse-grained groups [33]. Hot standby servers should be provisioned according to the full capacity of a data parallel group, determined by multiplying pipeline parallelism ( $PP$ ) by tensor parallelism ( $TP$ ). For instance, training a 530B GPT model requires 280 spare GPUs on standby, which results in an 11% increase in training costs [51]. Spare servers can potentially run small training jobs while on (non hot) standby to amortize cost. However, the job eviction latency needed to free these resources upon a failure can cause long stalls for large training jobs occupying thousands of GPUs.

The alternative approach is to continue training with the largest possible subset of functional resources. *Ideally, when  $x\%$  of GPU servers fail, training can continue at no less than  $(100 - x)\%$  of the fault-free throughput.* The simplest method, sometimes referred to as *elastic batching*, is to drop a whole data parallel (DP) group when a node fails [44, 72]. The remaining data parallel groups can proceed with the same parallelization scheme. While straightforward, this method has substantial drawbacks. A single node failure results in  $PP \times TP$  nodes going offline, decreasing the total throughput by  $1/DP$  (e.g., 17% when training a 1000B parameter GPT model [51]). Moreover, this requires reducing the training batch size or recompiling the program to optimize each data parallel group for a larger portion of the batch. This can disrupt the balance and efficiency of the entire training job.

Two recent projects have instead utilized pipeline parallelism for efficient training in the presence of failures without

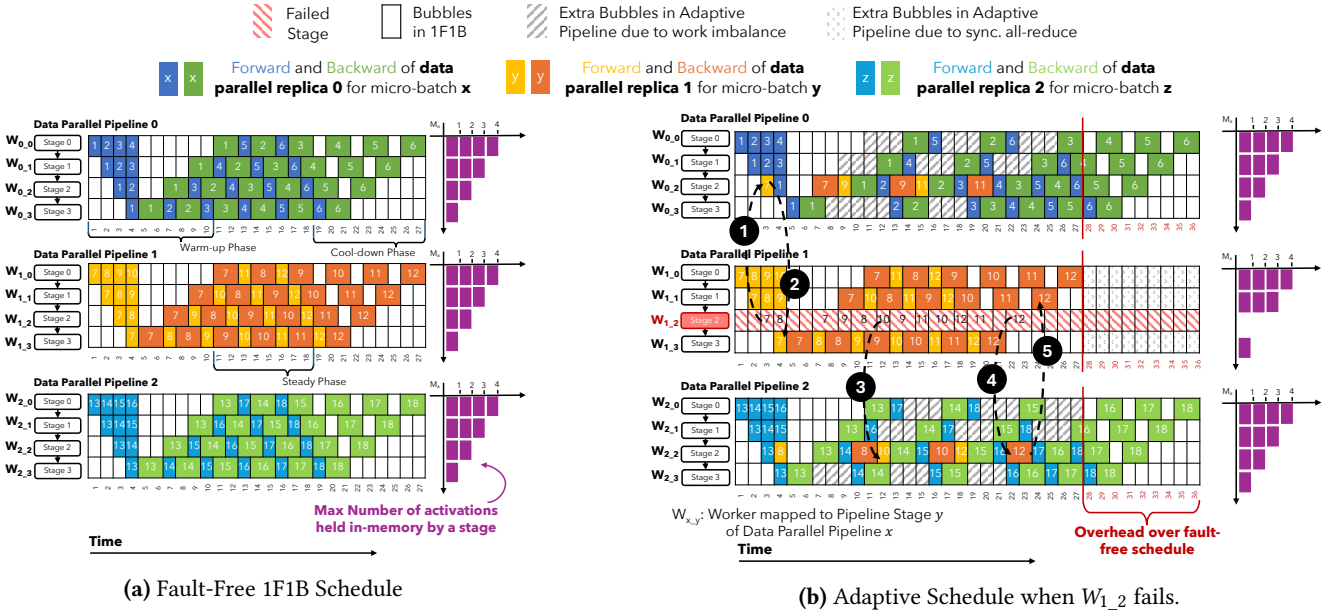


**Figure 3.** Hybrid-parallel training with 3 data-parallel pipelines, 4 pipeline stages, and 6 micro-batches per iteration. 3a shows a 1F1B fault-free schedule. 3b shows how *Adaptive Pipelining* re-routes micro-batches failed workers to functional peers.

spares. Bamboo [67] draws inspiration from RAID [55] and designs a pipeline for redundant computation (RC). Each pipeline stage is redundantly computed on two nodes, even in the fault-free case. When a node fails, its backup node steps up and computes the forward and backward passes of the failed node. Bamboo uses RC even in the absence of faults. While RC tries to hide some overhead in pipeline bubbles, its extra computational overhead still significantly drops training throughput (see Section 5). RC also replicates the state of each pipeline stage in two nodes, increasing GPU memory pressure and limiting its scalability. Finally, Bamboo needs to restart with a full reconfiguration from a checkpoint for as few as two failures, e.g., when two adjacent nodes fail.

Obleck [28] adapts pipeline parallelism for resilient execution but has no overhead in the fault-free case. It relies on pre-computed templates for pipeline parallelism. All templates are logically equivalent yet physically heterogeneous. Each template has a different number of stages, a different micro-batch configuration, and occupies a different number of nodes. A pipeline with failed node(s) is replaced with a new pipeline from a template that requires fewer nodes. However, templates with fewer nodes have lower training throughput. To avoid having the slowest pipeline slowdown the overall synchronous training job, Obleck attempts to distribute the global mini-batch proportionally to compute power. This is not always possible and the straggling pipelines will inflate training time. Moreover, each pipeline re-configuration is in the critical path of training and can become an overhead if nodes fail frequently. Re-configuration is also needed when nodes re-join. Finally, Obleck treats each heterogeneous

pipeline as a *black-box*. It fails to observe that there are bubbles across all pipelines that can help hide some or all of the overheads due to node failures.

### 3 SlipStream Techniques

SlipStream aims to support efficient distributed training in the presence of faults. It requires no spare servers and has no impact on model accuracy compared to fault-free training. SlipStream can tolerate multiple hardware failures and maintains training throughput proportional to the number of functional servers available. SlipStream is optimized for fast recovery as failures do not require significant re-shuffling of model parameters between functional nodes.

This section reviews the key SlipStream techniques: *Adaptive Pipelining*, *Decoupled BackProp*, and a *Staggered Optimizer*. Section 4 presents the SlipStream system design.

#### 3.1 Adaptive Pipelining: Working Around Failures

SlipStream exploits two key properties in hybrid-parallel training systems. First, there is *functional redundancy* across data-parallel pipelines. The GPUs that process the same pipeline stage hold identical parameters and only differ in the micro-batches they process. In Figure 2, for example, workers  $W_{0.2}$ ,  $W_{1.2}$ , and  $W_{2.2}$  are *peers* that hold identical parameters for stage 2 of the 4-stage pipeline. Second, there are bubbles (idle slots) in the pipeline schedule for each worker. The 1F1B pipeline schedule [50] in Figure 3a has 9 bubbles in the repeating 27-slot schedule for worker  $W_{0.2}$ .

*Adaptive Pipelining* exploits functional redundancy and bubbles by *dynamically re-routing micro-batches* from a failed

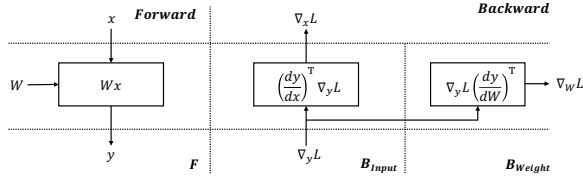


Figure 4. Forward and Backward pass for an operator.

worker to its functioning peers in other data-parallel pipelines. We aim to use the bubbles in peers’ schedules to process the micro-batches for the failed worker at low performance penalty. We evenly distribute micro-batches across all functional peers. Since all pipelines perform a synchronized all-reduce at the end of each iteration, load balancing ensures that no single worker (and thus pipeline) is overloaded, delaying the progress of the entire training iteration.

Figure 2 shows an example with three data parallel, 4-stage pipelines. Worker  $W_{1_2}$  fails. Upon detecting the failure, *Adaptive Pipelining* will redirect its input to workers  $W_{0_2}$  and  $W_{2_2}$ . These two peer workers will process micro-batches received from worker  $W_{1_1}$  in addition to their regular pipeline load. The output for these additional micro-batches will be sent back to worker  $W_{1_3}$ , the original recipient of the output of the failed worker  $W_{1_2}$ . All other workers operate as in the fault-free schedule. In essence, *Adaptive Pipelining* repairs the functionality of pipeline 1 by exploiting bubbles in the data parallel peers of failed worker  $W_{1_2}$ . Note that *Adaptive Pipelining* requires *no model parameter re-shuffling or re-partitioning across workers* in order to resume after a failure. Hence recovery is fast, unlike schemes like Oobleck that require re-configuring an entire pipeline upon a failure [28].

Figure 3 shows the detailed 1F1B schedule for the system in Figure 2. After the failure, the *forward pass* micro-batch 7 for failed worker  $W_{1_2}$  is re-assigned to its functional peer  $W_{0_2}$  at time step 3 (1). The subsequent output is forwarded back to worker  $W_{1_3}$  at time step 4 (2). Similarly, the *forward pass* of micro-batch 10 is re-routed to worker  $W_{2_2}$  at time step 12 (3). The *backward pass* operates similarly in the opposite direction. Worker  $W_{2_2}$  receives from worker  $W_{1_3}$  the gradients for micro-batch 12 at time step 22 (4). The output gradients are passed to worker  $W_{1_1}$  at time step 24 (5). The overall mathematical computation remains *unchanged* from the fault-free 1F1B schedule, ensuring that *Adaptive Pipelining* does not impact model convergence.

**The scheduling challenge:** In theory, the execution schedule of the two peer workers has enough bubbles to do the computations for failed node  $W_{1_2}$  as there are 18 idle slots in total in Figure 3a. However, these bubbles are concentrated in the warm-up and cool-down phase of the 1F1B schedule. *Adaptive Pipelining* needs to reroute micro-batches to peer workers  $W_{0_2}$  and  $W_{2_2}$  mostly in the middle of their steady-state schedule, which is optimized to be bubble-free

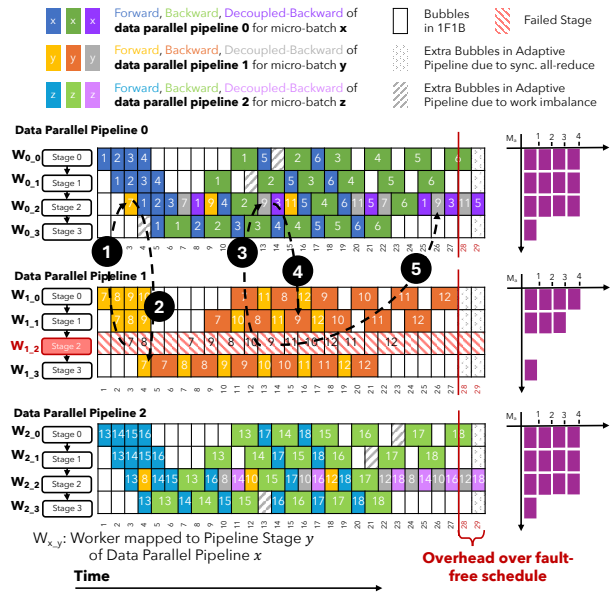


Figure 5. Optimized schedule with *Decoupled BackProp* when worker  $W_{1_2}$  fails.

for efficiency [50]. As shown in Figure 3b, this has a significant performance impact. The additional micro-batches to peer workers and the dependencies between forward and backward pass computations lead to 36 time steps per iteration. In other words, the failure of 8.3% of workers (1 out of 12) leads to a 33% slowdown in iteration time.

### 3.2 Decoupled BackProp: Filling Unused Bubbles

*Decoupled BackProp* addresses the scheduling problem of *Adaptive Pipelining*. It separates the backward pass into two distinct phases, allowing for more flexible scheduling of the extra load in the peers of a failed worker. Figure 4 shows that the backward pass calculates two distinct outputs: the gradients relative to the input ( $B_{Input}$ ) and the gradients relative to parameters (weights) for that pipeline stage ( $B_{Weight}$ ). Conventionally,  $B_{Input}$  and  $B_{Weight}$  are *coupled* as a unified calculation. *This coupling lengthens dependencies between pipeline stages*. The backward pass for stage  $i$  must wait for the completion of both  $B_{Input}$  and  $B_{Weight}$  from stage  $i + 1$ , despite stage  $i$  requiring only  $B_{Input}$  for its backward computations.  $B_{Weight}$  can be deferred to improve the overall pipeline schedule. Thus, *Decoupled BackProp* splits the backward pass into two distinct tasks.

Figure 5 explains how *Decoupled BackProp* reduces the overheads introduced by *Adaptive Pipelining*. It shows the same example as in Figure 3 with the addition of *Decoupled BackProp*. The forward pass for the micro-batch 7 is unchanged (1 and 2). However, instead of waiting on a *coupled* backward pass (both  $B_{Input}$  and  $B_{Weight}$ ) from the previous stage to complete, which causes a ripple effect of dependencies throughout the pipeline, subsequent stages

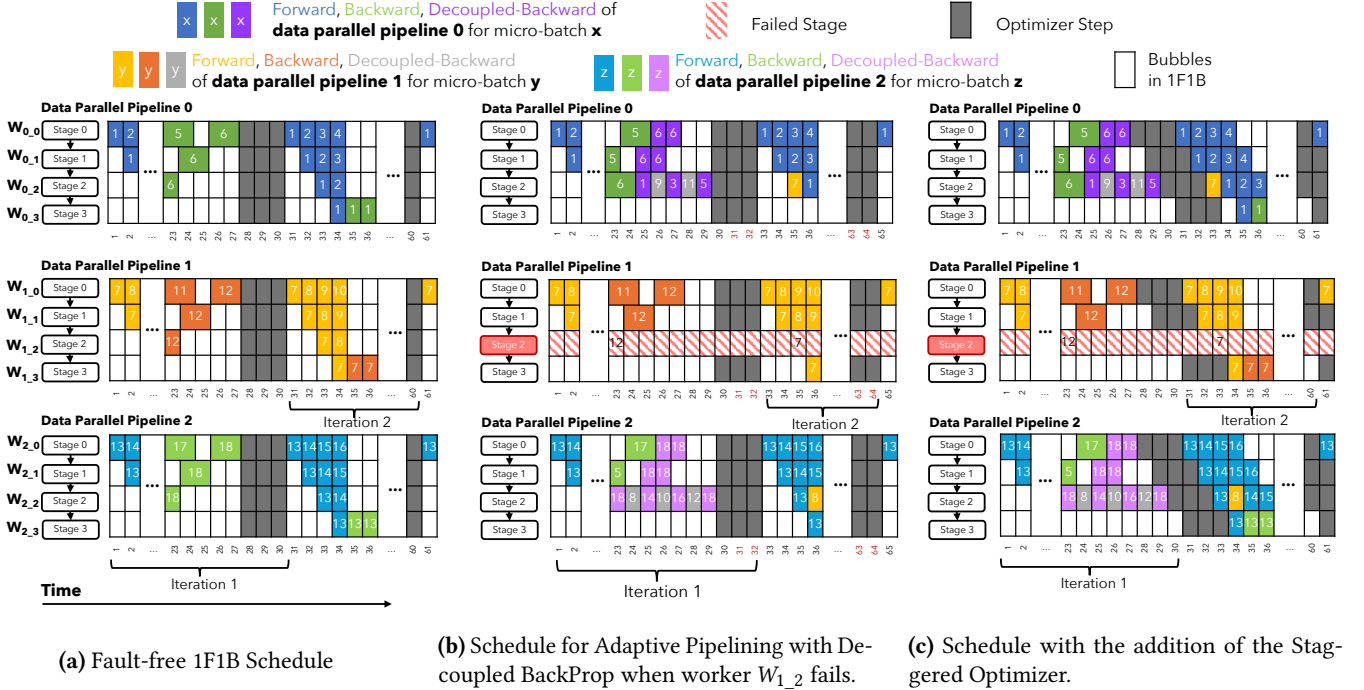


**Figure 6.** The Staggered Optimizer allows SlipStream to optimize pipeline schedule across training iterations.

can continue processing new micro-batches using just the  $B_{Input}$  from their predecessors. For example, worker  $W_{0.2}$  can run the backward pass for micro-batch 9 (3) and immediately pass the  $B_{Input}$  to worker  $W_{1.3}$  (4) without computing  $B_{Weight}$ .  $B_{Weight}$  is deferred to a later time (5) to reduce pipeline stalls, bringing the overall overhead down to just two time-steps (7.4% overhead with 8.3% failed workers).

Because  $B_{Weight}$  is dependence-free, it can largely be deferred until the end of the training iteration. Hence, we can take advantage of idle slots in the cool-down phase of the 1F1B schedule for  $B_{Weight}$  computations, freeing slots in the steady stage for the re-routed work of the failed worker. This enables SlipStream to absorb the additional computational demands imposed by failures with minimal overheads.

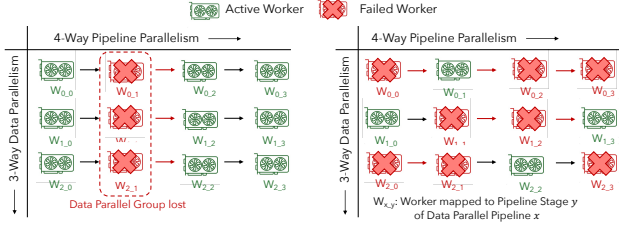
**The memory challenge.** Unfortunately, *Decoupled BackProp* increases memory pressure. Decoupling the computation of  $B_{Weight}$  requires that intermediate data is stored for potentially extended periods on each worker. For instance, as shown in Figure 5, decoupling the backward pass for micro batch 1 necessitates retaining its intermediate data until time step 25. To avoid memory exhaustion, SlipStream applies *Decoupled BackProp* selectively only when it can mitigate the overheads of *Adaptive Pipelining*. We also capitalize on the observation that memory imbalance exists among the pipeline stages [35]. To ensure that all pipeline stages are fully utilized, earlier stages need to allocate additional memory to process more forward micro-batches than later

stages [50]. By exploiting this available *surplus* memory, SlipStream can effectively offset some of the memory demands of *Decoupled BackProp* without incurring additional costs.

### 3.3 Staggered Optimizer: Accessing More Bubbles

*Decoupled BackProp* makes efficient use of the cool-down bubbles. However, as seen in Figure 6, the warm-up bubbles remain underutilized due to their placement *after* the synchronous optimizer step of the previous iteration. To exploit warm-up bubbles, we make the critical observation that optimizer steps for different pipeline stages are independent of each other. The *Staggered Optimizer* thus shifts the timing of the optimizer step across pipeline stages to better utilize the bubbles that occur during the warm-up phase of the subsequent training iteration. Effectively, this staggering provides SlipStream *more* bubbles in the cool-down phase to hide the overhead of compensating for failed workers.

Figure 6c shows how combining *Staggered Optimizer* with *Adaptive Pipelining* and *Decoupled BackProp* results in *zero overhead* over the fault-free 1F1B schedule in the running example. By staggering the optimizer step, later pipeline stages can move bubbles from the warm-up phase of the second iteration to the cool-down phase of the first iteration. Thus, peers that need to process additional micro-batches from failed workers within their steady-state schedule (i.e., workers  $W_{0.2}$  and  $W_{2.2}$ ) can further defer their weight gradient computations towards the cool-down phase. Workers for earlier stages (e.g.,  $W_{0.0}$  for stage 0) can continue with



(a) The loss of an entire DP group requires checkpoint restoration. (b) SlipStream can continue training if a functional worker exists per stage.

Figure 7. Example of SlipStream’s fault tolerance guarantees.

the optimizer step, ensuring that the entire pipeline does not stall. Worker  $W_{0_0}$  can start iteration 2 at *exactly the same time step as the fault-free 1F1B schedule*, even with failures.

Put together, these three mechanisms allow SlipStream to flexibly optimize the use of computational resources across pipelines, ensuring that each stage operates near its capacity and maintains consistent utilization throughout training.

### 3.4 Supporting Multiple Failures

SlipStream’s techniques support multiple failures. SlipStream guarantees continued training up to  $DP - 1$  simultaneous worker failures, where  $DP$  is the number of data-parallel pipelines, as one functional worker exists for each pipeline stage. SlipStream can probabilistically sustain more failures, as long as there is at least one functional worker per stage across all data parallel pipelines. Figure 7b shows how SlipStream can recover from more than  $DP - 1$  failures. Despite 8 simultaneous failures – *2/3 of the GPUs!* – SlipStream continues training.

As workers are repaired, SlipStream can re-insert them back into the adapted pipeline schedule, reducing the probability of high counts of concurrent failures. In the rare event that simultaneous failures affect a single data parallel group as shown in Figure 7a, SlipStream resorts to current resilience solutions: calculate an efficient hybrid-parallel scheme for the remaining nodes, configure it across all workers by restoring from a recent checkpoint, and resume training at the speed the new parallelism scheme allows.

**Multi-GPU Servers and Tensor Parallelism.** Training systems commonly employ servers with multiple GPUs. A favoured configuration involves HGX/DGX servers with 8 GPUs connected in an all-to-all manner using NVLink and NVSwitches [17]. Similar to Oobleck and Bamboo, we consider a whole server as the unit of failure. This approach is pragmatic because servicing even one faulty GPU board necessitates taking the entire server offline. Moreover, software faults, CPU issues, connectivity problems, and power or cooling issues can also incapacitate a whole server. We also need to account for the level of tensor parallelism. Most training systems apply tensor parallelism within a multi-GPU

server to leverage the high-bandwidth NVLink connections. In cases where tensor parallelism spans multiple servers, SlipStream, along with Oobleck and Bamboo, identifies the collective group of tensor-parallel servers as a unit of failure.

## 4 SlipStream Design

### 4.1 System Overview

SlipStream consists of three key components, the *Profiler*, the *Executors*, and critically the *Planner*.

**Profiler.** When a large training job is first submitted, SlipStream runs a short profiling job to collect key performance statistics such as the average micro-batch latency for the forward and backward passes, memory requirements for activations and gradients, and inter-node communication bandwidth. The profiling job executes a small number of training iterations, 100 by default, and typically takes a few minutes. These statistics are used by the *Planner*.

**Planner.** The *Planner* generates near-optimal schedules for the training job under various failure scenarios. It uses dynamic programming (DP) and mixed integer linear program (MILP) formulations that implement the SlipStream techniques (Section 3). We generate a pipeline schedule for each *number* of tolerated simultaneous failures. Each plan is agnostic to which specific worker(s) fail. It encodes the specific pipeline schedule including micro-batch assignment, the order of forward and backward tasks (e.g., *ForwardPass*, *BackwardWeightPass*), and the communication plan (e.g., *RecvActiv*, *SendGrad*, etc.). The plans are stored in distributed fault-tolerant storage (e.g., *etcd*) to be used by runtime *Executors*.

By default, we generate up to  $DP - 1$  plans, which accounts for the  $DP - 1$  simultaneous failures that SlipStream can always handle. Since SlipStream can probabilistically sustain many more failures, we can also generate plans for up to a user-defined fault tolerance threshold. The *Planner* runs relatively quickly, requiring 53 minutes to generate plans for up to 512 concurrent failures for a cluster of 2048 GPUs. Nevertheless, the training job can begin training in parallel as most plans will not be needed immediately.

**Executors.** SlipStream operates with an *Executor* on each GPU node, tasked with implementing the training plan specific to that node. Overseeing these Executors, a centralized *Coordinator* orchestrates the overall training operation by distributing the appropriate execution plans to each Executor. Additionally, the *Coordinator* actively monitors the status of all Executors to ensure their continuous operation. In the event of a failure, the *Coordinator* reassigns the tasks impacted by failure to the most suitable location, as advised by the *Planner* (refer to Section 4.2.1), and then directs the remaining *Executors* to resume training according to the updated plan that now reflects the updated count of non-operational workers. Training resumes from the iteration during which the failure was identified. If failures are not

promptly detected, restoring a checkpoint from remote storage may become necessary. To enhance reliability, the *Coordinator* itself is safeguarded against failures through active replication.

## 4.2 SlipStream Planner

Given the cluster configuration, training job, profiling statistics, and set of failed workers, the *Planner* calculates a valid pipeline schedule that minimizes the training iteration latency using the fault-free workers. The *Planner* uses two phases, *Normalization* followed by *Solution*.

SlipStream generates an execution plan for a given number of failures, regardless of which worker(s) fails, as solving ILP problems for the combinatorial number of possible failure locations is intractable. The first phase *normalizes* the specific failures by migrating failed nodes to a pre-determined and ideal set of locations within the pipeline schedule. For example, if any single node fails in the example in Figure 7, the *Planner* will always swap the node with an ideal location, e.g.  $W_{2,3}$ . The *Planner* generates a mapping of the ideal migration locations for each possible number of simultaneous failures. Unlike current solutions which require a complete reconfiguration of a data-parallel pipeline, normalization only requires a point-to-point copy of model parameters to swap the location of two workers in the pipeline for each failure. The *Solution Phase* leverages an MILP to derive an optimized schedule for each normalized case.

**4.2.1 Normalization Phase.** The intuition behind the Normalization Phase is to a) distribute failures across different peer groups (to maximize fault tolerance and load balance extra work across peer groups) and b) move failures to later pipeline stages with more bubbles (to maximize the opportunity to hide overheads).

Normalization relies on dynamic programming (DP) to determine the ideal pipeline location to migrate faults for given a number of failures. We use a DP algorithm as it can greedily determine the ideal migration strategy with very low runtime ( $O(NF^2)$  complexity for all solutions up to  $F$  failures with  $N$  stages per pipeline). The DP algorithm is based on a model that calculates the cost in terms of the extra bubbles used to accommodate re-routed micro-batches.

**DP Formulation.** Given the total number of failures to handle,  $F$ , and the total number of pipeline stages within a data parallel pipeline,  $N$ , the DP algorithm returns a list  $R$  of length  $N$ , such that  $\sum_i R[i] = F$ . Each index  $R[i]$  specifies the ideal number of failures that is assigned to pipeline stage  $i$  across all data parallel pipelines; the specific pipeline assignment does not affect performance and can be arbitrary. For example, if  $R[3] = 2$  for the example in Figure 7a, the ideal migration would be to swap the failed nodes with any two nodes in stage 3, for example  $W_{0,3}$  and  $W_{2,3}$ .

---

### Algorithm 1 Normalization Phase DP Algorithm

---

```

1:  $N \leftarrow$  Number of pipeline stages.
2:  $F \leftarrow$  Total number of failures.
3:  $C \leftarrow$  an  $N \times (F+1)$  array ▷ Costs
4:  $A \leftarrow$  an  $N \times (F+1)$  array ▷ Assignments
5: for  $i \in \{0, \dots, N-1\}$  do
6:   for  $f \in \{0, \dots, F\}$  do
7:     if  $i == 0$  then
8:        $C[i][f] = cost(i, f)$ 
9:        $A[i][f] = [f]$ 
10:    else
11:       $C[i][f] = \min_{x \leq f} (C[i-1][f-x] + cost(i, x))$ 
12:       $x = \arg \min_{x \leq f} (C[i-1][f-x] + cost(i, x))$ 
13:       $A[i][f] = concat(A[i-1][f-x], x)$ 
14:    end if
15:  end for
16: end for
17:  $R = A[N-1][F]$ 
18: return  $R$ 

```

---

For each DP step,  $C[i][f]$  represents the total cost, in terms of bubbles used, to handle  $f$  failures at all stages between 0 and  $i$ . Meanwhile, each  $A[i][f]$  contains a list that denotes the portion of the  $f$  failures assigned to each stage from 0 to  $i$ , as described for  $R$  – in other words  $len(A[i][f]) = i + 1$ . Each DP step uses a recurrence relation that aims to minimize the cost of handling  $f$  failures within the first  $i$  pipeline stages across all of the data parallel pipelines, while  $A[i][f]$  denotes the assignment of failures that achieves this cost. The ideal assignment to handle  $F$  failures across all workers is simply  $R = A[N-1][F]$ .

To estimate the cost,  $cost(i, x)$  is a function that returns the extra bubbles used to handle the extra micro-batches from  $x$  failures in the  $i$ -th stage (i.e., peer group). While we can use the MILP described in Section 4.2.2 to estimate the cost, the *Planner* can also rely on a heuristic to estimate the cost in order to avoid longer solve times (as Algorithm 1 requires  $O(NF)$  calls to the cost function). The heuristic captures the benefit of the techniques described in Section 3. It creates a pipeline schedule that is similar to 1F1B, except that the heuristic’s 1F1B backward pass only schedules  $B_{input}$ . Then, when there exists a gap (both in terms of time and memory) that is able to fit  $B_{weight}$  (or the  $F$  and  $B_{input}$  stages are exhausted),  $B_{weight}$  operations are scheduled opportunistically.

**4.2.2 Solution Phase.** Next, the *Planner* uses the normalized failure locations and the profiled statistics as inputs to an MILP which performs schedule optimization. At a high level, the MILP determines how to schedule re-routes micro-batches across peers of a failed worker alongside regular



micro-batches in those peers (*Adaptive Pipelining*). The formulation accounts for the latency for communicating gradients across workers, task dependencies in forward and backward passes, and the memory usage in each worker. The definition of task dependencies also allows the solution to leverage *Decoupled BackProp* and *Staggered Optimizer* techniques.

**MILP Formulation.** We aim to minimize the makespan of a single training iteration which is repeated throughout the training process, while the constraints are task dependencies and the memory capacity of workers.

**Notation.** An operation within a training iteration can be explicitly identified across workers using a 5-tuple  $(i, j, k, c, k_s)$ .  $i$  represents the pipeline stage within each data parallel pipeline, while  $k$  represents the operation’s original data parallel pipeline (prior to failures).  $j$  is the micro-batch ID in the training iteration.  $c$  identifies the different operations for each micro-batch,  $c \in \{F, B_{input}, B_{weight}\}$ . Finally,  $k_s$  denotes the *peer* pipeline in the event that a micro-batch *originally* intended for  $k$  runs on  $k_s$  (note that  $k$  can equal  $k_s$ ). For example, a micro-batch originally intended to execute on  $W_{2,3}$ , but was re-routed to a peer  $W_{1,3}$  in Figure 7, would have  $i = 3, k = 2$ , and  $k_s = 1$ . Thus,  $(i, k_s)$  uniquely identifies the worker for a given operation.

**Inputs.** The MILP takes as input the micro-batch to worker assignments in an iteration. Specifically, the *Planner* takes the normalized failure locations and assigns all micro-batches corresponding to failed workers evenly across peer workers within the same peer group, alongside the original (non-peer) micro-batches. Thus, the *Planner* produces a binary mapping  $S_{i,j,k}^{k_s} \in \{0, 1\}$ , which indicates if a micro-batch  $(i, j, k)$  should be executed on pipeline  $k_s$ . Note that  $S_{i,j,k}^{k_s} = 1$  if the micro-batch executes on the original pipeline. We ensure that each operation is assigned only one pipeline, i.e.,  $\sum_{k_s} S_{i,j,k}^{k_s} = 1$ .

The MILP also takes as input profiled statistics. First,  $T_c$  represents the computational time for each operation  $c$ .  $T_{comm}$  represents the communication latency to send activations or gradients across workers<sup>1</sup>. Next, the MILP requires the *change* in memory utilization on worker  $(i, k, k_s)$  caused by executing an operation  $(i, j, k, c, k_s)$  as  $\Delta M_{i,j,k,c}^{k_s}$ .

$$\Delta M_{i,j,k,c}^{k_s} = \begin{cases} A_B & , \text{ if } c = F \text{ and } S_{i,j,k}^{k_s} = 1 \\ A_B - A_{B_{input}} & , \text{ if } c = B_{input} \text{ and } S_{i,j,k}^{k_s} = 1 \\ -A_{B_{weight}} & , \text{ if } c = B_{weight} \text{ and } S_{i,j,k}^{k_s} = 1 \\ 0 & , \text{ otherwise} \end{cases}$$

Here,  $A_B$  is the profiled size of activation stored at the end of forward pass.  $A_{B_{input}}$  and  $A_{B_{weight}}$  is size of the activation stored at the end of backward-input and backward-weight

pass, respectively. Upon completion of backward-input pass and backward-weight pass, we free activation  $A_{B_{input}}$  and  $A_{B_{weight}}$  respectively.

**Variables.** The goal of the MILP is to identify the exact ordering of operations, which can be used to generate a pipeline schedule. To do this, we introduce an ordering variable  $O_{(i,j,k,c,k_s) \rightarrow (i',j',k',c',k'_s)} \in \{0, 1\}$  between each pair of operations  $(i, j, k, c, k_s)$  and  $(i', j', k', c', k'_s)$ . Each variable is 1 if  $(i', j', k', c', k'_s)$  is scheduled any time after  $(i, j, k, c, k_s)$  and 0 otherwise. Ordering is only required within a stage, and between computation phases of same micro-batch (e.g., between the  $F$  and  $B_{input}$  pass). Finally, we define the set of variables  $E_{i,j,k,c}^{k_s}$  as the ending time of operation  $(i, j, k, c, k_s)$ .

**Objective.** The goal of the MILP is to minimize the makespan of a single training iteration (which is repeated throughout the training process). This can be done by determining the sequence and time of operations through the training pipeline via the sets of variables  $O$  and  $E$ . This objective can thus be formulated as:

$$\min_{O,E} \quad \max_{i,j,k,k_s} E_{i,j,k,B_{weight}}^{k_s} \quad (1)$$

Here,  $\max_{i,j,k,k_s} E_{i,j,k,B_{weight}}^{k_s}$  represents the end time of the *last* operation in the iteration, representing the makespan.

**Constraints.** The constraints applied to the objective are the following.

*Cross-Stage Dependencies.*

$$E_{i,j,k,F}^{k_s} \geq S_{i,j,k}^{k_s} \times \left( \sum_{\hat{k}} (E_{i-1,j,k,F}^{\hat{k}} \times S_{i-1,j,k}^{\hat{k}}) + T_{comm} + T_F \right) \quad (2)$$

$$E_{i,j,k,B_{input}}^{k_s} \geq S_{i,j,k}^{k_s} \times \left( \sum_{\hat{k}} (E_{i+1,j,k,B_{input}}^{\hat{k}} \times S_{i+1,j,k}^{\hat{k}}) + T_{comm} + T_{B_{input}} \right) \quad (3)$$

Equation 2 specifies the dependency of a given micro-batch’s forward pass on previous pipeline stages (e.g., stage 0 must execute before stage 1). Similarly, Equation 3 specifies the reverse dependency for the backward pass (e.g., stage 1 must execute before stage 0).

*Same-Stage Dependencies.*

$$E_{i,j,k,B_{weight}}^{k_s} \geq S_{i,j,k}^{k_s} \times (E_{i,j,k,B_{input}}^{k_s} + T_{B_{weight}}) \quad (4)$$

Equation 4 allows the MILP to reason about *Decoupled BackProp*, specifying that  $B_{input}$  must precede  $B_{weight}$  for a given micro-batch within a worker.

*No Overlapping Computations.*

$$E_{i,j',k',c'}^{k'_s} \geq E_{i,j,k,c}^{k_s} + T_{c'} - \infty(1 - S_{i,j,k}^{k_s} \times S_{i,j',k'}^{k'_s} + O_{(i,j,k,c,k_s) \rightarrow (i,j',k',c',k'_s)}) \quad (5)$$

Equation 5 adds a dependency constraint which specifies that two different operations cannot overlap in time if they are executed on the same worker. For example, if operation

<sup>1</sup>We use a single value as activations and gradients are the same size.

$(i, j', k', c', k'_s)$  is scheduled after  $(i, j, k, c, k'_s)$ , they both execute on worker  $(i, k'_s)$  and thus  $(i, j', k', c', k'_s)$  must begin after  $(i, j, k, c, k'_s)$  ends.

*Memory Constraint.*

$$M_{Limit} \geq \Delta M_{i,j',k',c'}^{k'_s} + \sum_{j,k,c} \Delta M_{i,j,k,c}^{k'_s} \times O_{(i,j,k,c,k'_s) \rightarrow (i,j',k',c',k'_s)} \quad (6)$$

Finally Equation 6 calculates the activation memory required at any given time on worker  $(i, k'_s)$ , and constrains operations such that the total memory is below an  $M_{Limit}$  to avoid OOMs.

### 4.3 Implementation

We implemented SlipStream on top of DeepSpeed [60] and made the following additions to DeepSpeed to support SlipStream.

**Rerouting micro-batches to data parallel peers.** To handle the dynamic rerouting of micro-batches following node failures, we introduce two new and complementary communication operators: `ReRouteAct` and `ReRouteGrad`. Positioned at the end of a pipeline stage, `ReRouteAct` normally acts as a pass-through, transmitting computed intermediate activations to the next stage within the same data parallel pipeline. Conversely, `ReRouteGrad`, located at the beginning of a stage, typically forwards gradients backward through the pipeline. When a subsequent stage fails, `ReRouteAct` redistributes the micro-batches across the remaining peers in a round-robin fashion, while `ReRouteGrad` adjusts the gradient distribution to ensure that both the forward and backward processes of a micro-batch are handled by the same peer. This strategy maintains operational continuity in SlipStream under fault conditions, mirroring fault-free execution semantics. These operators are integrated as *pipeline instructions* within the DeepSpeed execution engine.

**Decoupling Back Propagation in DeepSpeed.** Our implementation of *decoupled backpropagation* within DeepSpeed centers around intercepting the weight gradient computations traditionally performed during the backpropagation phase. These computations are temporarily held in a newly created in-memory structure known as *WeightGradStore*, enabling SlipStream to defer weight gradient computation. To facilitate this, two new *pipeline instructions* have been introduced into DeepSpeed’s execution engine: `InputBackwardPass` and `WeightBackwardPass`. These instructions are incorporated into SlipStream’s execution plan and are then processed by DeepSpeed’s execution scheduler, effectively managing the distinct phases of backpropagation.

**Bypassing Optimizer Synchronizations.** In DeepSpeed, each training iteration concludes with an all-reduce collective to synchronize gradients across data parallel peers, followed by a series of validation checks at each pipeline stage

to ensure numerical stability, such as monitoring for gradient overflow. If any stage identifies an issue that could compromise numerical stability, the optimizer step for that iteration is omitted to avoid exacerbating the problem. Upon successful validation, the optimizer step is executed for each stage, and the training progresses to the next iteration in a synchronized manner across all stages.

In contrast, SlipStream employs a staggered timing approach for the optimizer steps across different pipeline stages to enhance scheduling efficiency. This method of staggering is not conducive to cross-stage synchronization for validating numerical stability prior to executing the optimizer. To accommodate staggered execution while maintaining validation integrity, numerical validations are shifted from a pre-step to a post-step process. Following the all-reduce collective, each stage immediately conducts its own *local* validation checks but does not wait for downstream stages to complete their validations. Each stage proceeds with its optimizer step based on its individual validation results and those of preceding stages. If a downstream stage fails its validation, a rollback is initiated across all stages before advancing to the next iteration. Notably, for many optimizers, including the widely-used AdamW [46], such rollbacks do not entail additional memory costs because the operations involved are arithmetically reversible. This adjustment allows SlipStream to retain the advantages of staggered operations while protecting the training process from potential instabilities.

## 5 Evaluation

### 5.1 Experimental Setup

**Cluster Setup.** We performed real-world experiments on a cluster of 32 NVIDIA A100 80GB GPUs in Azure. Specifically, we used four `Standard_NC96ads_A100_v4` instances, each with 8 GPUs, 96 vCPUs, and 880 GB of host memory. Each node has an 600 GB/s NVLink intra-node interconnect, as well as a 640 Gbps inter-node interconnect over 8 NICs. We performed scalability experiments using a simulator, which we present and validate in Section 5.3.

**Baselines.** We compared SlipStream to the two state-of-the-art baselines discussed in Section 2.3 – Bamboo [67] and Oobleck [28] – with all of their respective optimizations enabled. We report the *fault-free* throughput achieved by DeepSpeed [60] using an 1F1B pipeline schedule [50]. All baselines train on the same Azure cluster.

**Workloads.** We evaluated all systems using the Megatron [64] implementation of GPT-3 [9]. We used three GPT-3 sizes: Medium (350M), 3.35B, and 6.7B. We used (PP, DP) degrees of (2, 16), (4, 8), and (8, 4) for the Medium, 3.35B, and 6.7B models, respectively. All models used a TP degree of 1. We trained on wikitext [48] using (batch, micro-batch) size of (8192, 8), (1024, 1), and (1024, 1) for the Medium, 3.35B, and

**Table 1.** Normalized training throughput with increasing failure rates. Fault-free training represents 1.00, hence higher is better. Bamboo ran out of memory for GPT-3 3.35B and 6.7B.

Systems	GPT-3 Medium			GPT-3 3.35B			GPT-3 6.7B		
	6h	2h	30m	6h	2h	30m	6h	2h	30m
Bamboo [67]	0.71	0.69	0.55	OOM	OOM	OOM	OOM	OOM	OOM
Oobleck [28]	0.99	0.92	0.71	0.98	0.90	0.66	0.93	0.87	0.52
SlipStream	0.99	0.92	0.81	0.98	0.95	0.85	0.97	0.91	0.66

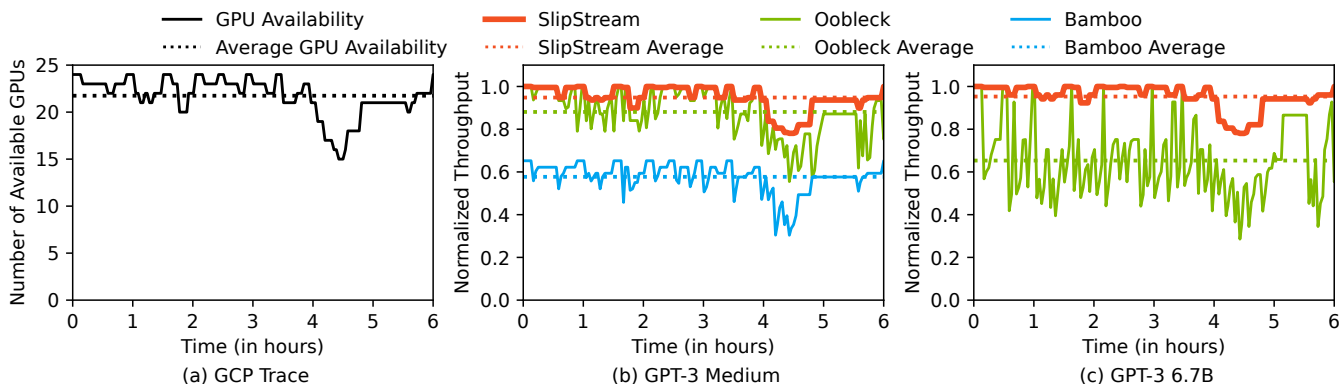


**Figure 8.** Training throughput, normalized to the fault-free case, for the GPT-3 Medium and GPT-3 6.7B models over the GCP trace. In 8b and 8c, the dashed lines represent the average training throughput achieved by each system within the 6h period.

6.7B models, respectively. Unless otherwise noted, all real-world experiments ran for 6 hours.

## 5.2 Training Throughput Under Failures

**How well does SlipStream handle failures compared to baselines?** For each 32-GPU training job on Azure, we instrumented a random GPU to fail at regular and increasing intervals: 6 hours, 2 hours, and 30 minutes, which is representative of real-world failure rates [29, 74], starting at the beginning of the training job ( $t = 0$ ). Note that we treat each individual GPU as a worker. Table 1 shows the average training throughput achieved by each system across models and failure rates normalized to the *fault-free* throughput achieved by DeepSpeed (1.00). Note that GPUs are not replaced after failure, hence the total number of workers monotonically declines throughout each experiment. With a failure every 30 minutes, the percentage of functional GPUs by the end of the 6 hour run is 62.5%. Hence, we expect the average throughput with a failure every 30min to be relatively modest compared to the fault-free case.

Because Bamboo relies on redundant computation, it rapidly exhausts GPU memory with its additional copy of model states and activations. Hence, Bamboo fails to train the two larger models. Even for the smallest model, redundant computation introduces significant throughput degradation. A single GPU failure (3% of total GPUs) in the 6h job causes a 29% throughput drop. Bamboo actually penalizes fault-free

execution by nearly the same percentage compared to DeepSpeed. Oobleck can handle all model sizes and achieves significant throughput improvements over Bamboo. However, as the frequency of failures and model size increase, Oobleck’s performance degrades. As failures increase, Oobleck’s heterogeneous pipelines become more imbalanced, degrading the throughput of the synchronous training job. As the model size increases, the latency of reconfiguring all of the stages in the pipeline with the failed GPU gets higher.

SlipStream is able to efficiently continue training under failures, out-performing or matching the throughput of both baselines across all models and failure rates. *Adaptive Pipelining*, *Decoupled BackProp*, and *Staggered Optimizer* are effective in optimizing the use of compute and memory resources across peers of failed GPUs. Moreover, SlipStream recovers from a failure quickly as it migrates model parameters to only a single GPU during normalization (see Section 4.2.1). Under frequent failures (every 30m) and no repairs, SlipStream achieves 85% and 66% of the fault-free training throughput for GPT-3 3.35B and 6.7B respectively. SlipStream outperforms Oobleck and Bamboo by up to 1.29 $\times$  and 1.46 $\times$ , respectively for these experiments. Note that, unlike Bamboo, both SlipStream and Oobleck introduce no penalty over DeepSpeed for fault-free execution.

**What is SlipStream’s throughput advantage in an realistic training scenario?** Next, we evaluated a realistic

**Table 2.** Gap between real-world and simulated throughput across various models and failure rates.

Models	Fault-Free	6h	2h	30m
GPT-3 Medium	-0.87%	+5.98%	-1.93%	-1.48%
GPT-3 3.35B	-0.13%	-1.58%	+2.12%	-1.90%
GPT-3 6.7B	+3.94%	+2.71%	-1.86%	-0.85%

training scenario where GPUs fail and re-join based on a real-world trace. We used a trace of node failures/repairs from GCP instances used by Bamboo [67]. We observed similar results for Bamboo’s AWS trace, but omitted the plots due to space constraints. We replayed the events in the GCP trace over a 6h training run on our Azure cluster. At the time of the experiment, we had 24 GPUs available (instead of 32 GPUs). Figure 8 shows the number of available GPUs over time according to the trace (max 24, min 15).

Figure 8 also plots the training throughput achieved by Bamboo, Oobleck, and SlipStream replaying the trace for a GPT-3 Medium and GPT-3 6.7B training job. Solid lines represent instantaneous training throughput, while dashed lines show the average training through for each system over the 6h period. Bamboo cannot train GPT-3 6.7B due to memory pressure. SlipStream achieves a 1.64 $\times$  higher performance (average throughput) compared to Bamboo on GPT-3 Medium and a 1.46 $\times$  higher performance than Oobleck on GPT-3 6.7B. As discussed above, Bamboo suffers from the overheads of redundant computations. Oobleck requires large stalls due to parameter re-shuffling both when GPUs fail and when they rejoin, causing frequent and large drops in throughput. Meanwhile, during periods of stability, Oobleck suffers from imbalanced heterogeneous pipelines as discussed above. SlipStream provides the highest and most consistent training throughput across all portions of the trace.

### 5.3 SlipStream Scalability

Since we do not have access to a cluster of thousands of GPUs, we built a simulator that can calculate the training throughput of a model and cluster configuration, given an execution plan. The simulator uses real-world profiled statistics for each pipeline operation of the respective model. To demonstrate that the simulator yields accurate results, Table 2 shows the gap between the simulated throughput and measured real-world throughput on Azure across different failure rates for the three GPT-3 models. The maximum difference is 5.98%. These differences arise due to minor fluctuations in the execution time of NCCL collectives, which do not cause impactful discrepancies when evaluating SlipStream.

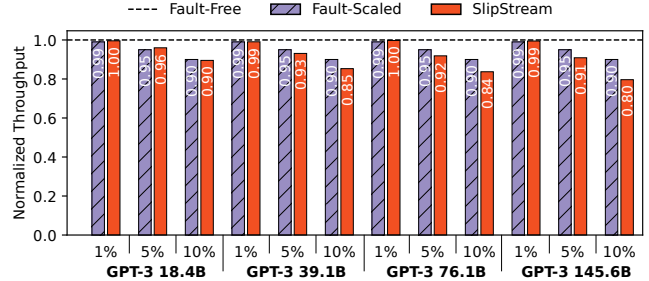


**Figure 9.** Simulated throughput of SlipStream as model size increases, normalized to the simulated fault-free 1F1B throughput. The Fault-Scaled throughput is the fault-free throughput scaled by the percent of non-failed GPUs.

### How well does SlipStream scale to large clusters and models?

Using the simulator, we explored how well SlipStream handles failures for large models training on larger clusters. Figure 9 shows of the simulated throughput achieved by SlipStream across four different GPT-3 models with up to 145.6B parameters, normalized to the simulated fault-free throughput achieved by DeepSpeed’s 1F1B schedule. We also show the *fault-scaled* throughput, which is obtained by multiplying the fault-free throughput by the percent of non-failed GPUs. Note that we report the steady-state throughput with 1%, 5%, and 10% failed GPUs, not the throughput as some number of GPUs fails and rejoins. We simulated a cluster of (# GPUs, # stages per pipeline, and # pipelines) = (256, 8, 32), (512, 16, 32), (1024, 32, 32) and (1536, 64, 24) for the 18.4B, 39.1B, 76.1B, and 145.6B model, respectively, which reflect the larger cluster sizes needed to train large models.

SlipStream is effective at achieving high throughput across failure rates and model sizes. For the case of 1% failures (higher reliability), SlipStream handles failures at or better than the fault-scaled throughput across all models and cluster sizes, often with zero degradation. The bubbles in peer workers are more than sufficient to efficiently execute the work for failed GPUs using SlipStream’s optimizations (see Figure 6). As the number of failed GPUs increases, SlipStream is still able to sustain high throughput. At 5% GPU failures, SlipStream achieves comparable performance to the fault-scaled throughput. Even at a large 10% failure rate (e.g., 154 failed GPUs for GPT-3 145.6B), SlipStream enables clusters to continue training while only observing between 0.5% and 11.5% degradation to the fault-scaled case. This suggests that SlipStream will be effective for training jobs in supercomputing-scale clusters with dynamic resource availability [23, 32, 79].

### 5.4 SlipStream Performance Breakdown

**How does each of SlipStream’s techniques contribute to performance?** To understand the benefit (and necessity) of each of the SlipStream techniques described in Section 3, we performed an ablation study by repeating the real-world

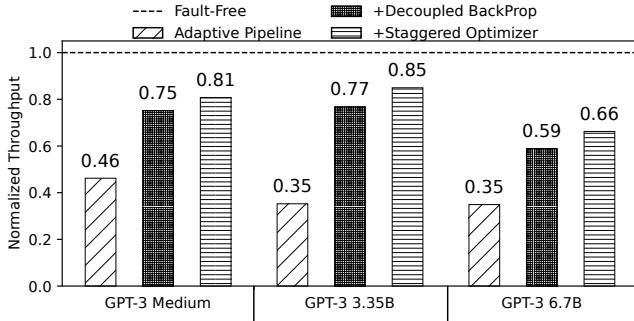


**Figure 10.** The contribution of the three optimization techniques to SlipStream’s training throughput.

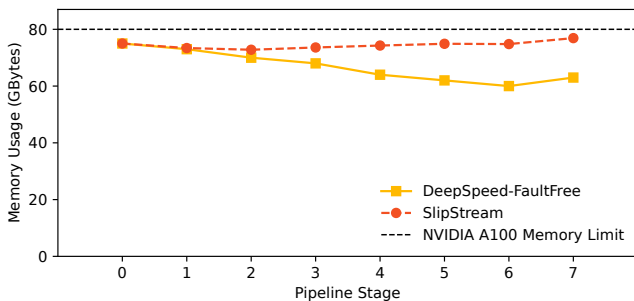


**Figure 11.** Memory utilization for SlipStream across pipeline stages for GPT-3 6.7B with 30m failure rates compared to DeepSpeed (failure-free). The dashed line shows the 80GB memory capacity of the A100 GPU.

experiment on the Azure cluster with the GPT-3 models and 30min failure frequency. We modified the MILP formulation in the *Planner* to progressively enable optimizations. Figure 10 shows the throughput achieved in each step of the study, normalized to the fault-free throughput.

*Adaptive Pipelining* allows SlipStream to continue training in the face of failures, but suffers from a large throughput degradation due to overheads caused by extra work in the peers of failed workers. By adding *Decoupled BackProp*, SlipStream boosts the training throughput by 63% to 118% by using bubbles in the cool-down phase of the pipeline schedule to mask this overhead (see Figure 3b). The addition of the *Staggered Optimizer* further improves throughput by 7% to 11% as it allows the use of bubbles from the warm-up phase of the pipeline schedule.

**Can SlipStream efficiently exploit unused GPU memory?** SlipStream makes the key insight that GPU memory capacity is not uniformly utilized throughout the pipelined execution. Later pipeline stages inherently use less GPU memory. *Decoupled BackProp* utilizes this free GPU memory as a buffer to defer  $B_{weight}$  computations (see Figure 5). To explore this in more detail, we analyzed the real-world training

**Table 3.** SlipStream *Planner* latency (in seconds) to find optimized schedules for up to 25% of failed GPUs.

DP Degree	PP Degree					
	2	4	8	16	32	64
2	5.24	5.41	15.48	42.73	129.57	459.57
4	7.65	8.62	24.48	59.75	190.54	719.4
8	8.56	9.57	30.74	81.42	294.21	1038.2
16	11.84	13.8	51.53	116.8	452.98	1721.45
32	11.71	14.87	67.24	278.64	942.42	3153.07

of the GPT-3 6.7B model with a 30m failure interval as in Section 5.2. Figure 11 shows the peak GPU memory utilization across the 8 stages of a pipelined execution, compared to the memory utilization of the failure-free DeepSpeed baseline.

DeepSpeed, and any system that uses a pipeline schedule similar to 1F1B, does not fully utilize GPU memory, especially in later pipeline stages [50]. This is because GPU workers that execute earlier pipeline stages must store a larger number of intermediate results, as shown in Figure 3. Figure 11 shows how SlipStream exploits this opportunity and uniformly utilizes nearly all GPU memory to optimize pipelined execution. The MILP formulation is able to carefully model and manage the additional memory requirements within GPU memory constraints and avoid memory exhaustion.

**What is the overhead of SlipStream’s Planner?** To understand how fast the *Planner* can generate optimized schedules for large clusters, Table 3 shows the time required to generate all necessary schedules for up to 25% of node failures across various parallelism strategies. Recall that the user can configure a smaller or larger fault-tolerance threshold. The reported latency includes both *Planner* phases. We report the results using Gurobi MILP solver [22] running on an 96-core CPU. We can generate all solutions to support up to 512 failures in the 2048-GPU case ( $DP = 32$ ,  $PP = 64$ ) within 3153 seconds (52.5 minutes). Given that the training time for large models on thousands of GPUs is measured in weeks [32, 52, 65], the *Planner*’s latency is insignificant.

## 6 Related Work

**Parallel Training.** Data parallelism [11, 15, 38] is a widely utilized mode of parallelism that distributes the dataset across different partitions for processing. In this mode, the learned weights are synchronized via either an all-reduce approach [11] or by using parameter servers [12, 31, 41]. Alternatively, model parallelism [37, 63, 64] involves distributing the components of a deep neural network (DNN) model across multiple GPU devices, allowing each device to handle a specific subset of the model’s parameters for all input data. Recently, pipeline parallelism [26, 35, 42, 45, 50] has emerged as a technique for training large models by dividing the model’s layers among different workers and utilizing microbatches to

efficiently use the available computational resources. Prominent deep learning training frameworks like PyTorch [57], DeepSpeed [60], and Megatron [51] have adopted hybrid-parallelism, an approach that integrates data parallelism, model parallelism, and pipeline parallelism. This integration facilitates training on a massive scale while enhancing computational and memory efficiency. Additionally, DeepSpeed introduces ZeRO-style [36, 58, 59, 61, 77] data parallelism, which strategically partitions model states across GPUs, coordinating via communication collectives to synchronize parameters as needed.

**Optimizing Hybrid-Parallel Training.** Improvements in hybrid parallelism are extensively studied in the context of ML training [26, 35, 36, 42, 43, 45, 50, 51, 60, 77, 78]. Alpa [78] automatically optimizes inter- and intra-operator parallelism using a hierarchical ILP formulation. Tofu [70] uses DP to optimally partition tensor operations in a single node. FlexFlow [30] uses a randomized search algorithm to quickly find parallelism strategies. TensorOpt [10] introduces a DP that can optimize parallelism for multiple resource dimensions (e.g., memory and compute). Piper [66] proposes a two-level DP algorithm to find optimal hybrid parallelism strategies. SlipStream uses a DP algorithm and an MILP which exploit key functional redundancies in hybrid parallelism to explicitly improve training throughput under failures.

**Elastic Training.** Elastic training systems can dynamically adjust the resources allocated to a training job. Both Horovod [62] and Torch Distributed [43] provide mechanisms to modify the number of workers, but require either a restart from a checkpoint or an expensive re-shuffling of model parameters. CoDDL [27], Optimus [56], OASIS [5], and Themis [47] are ML cluster schedulers that can dynamically allocate resources across multiple DNN training jobs. Or et al. [54] auto-scale the number of workers for a training job. Varuna [3] provides elastic training by leveraging spot instances, but requires restarts from checkpoints to handle unexpected preemptions. While some elastic training systems can affect model consistency by changing important hyperparameters such as batch size and learning rate, SlipStream ensures that operations are mathematically consistent regardless of the number of failures.

**Fault-tolerant Training.** DNN training systems widely leverage checkpoints as the basic mechanism for fault recovery [6, 23, 29, 32, 39, 60, 71, 79]. While *naive* checkpointing can lead to training stalls, recent work aims to reduce these overheads. CheckFreq [49] dynamically adapts the checkpointing frequency to reduce overheads. Check-N-Run [18] quantizes in-frequently updated embedding table checkpoints for recommendation models. Gemini [73] introduces checkpoint traffic scheduling across the storage hierarchy (local CPU memory, remote CPU memory, and

remote persistent storage). Megascale [32] alleviates the storage bottleneck during recovery by sharing data between corresponding GPU workers across data parallel groups.

Two recent projects have proposed to utilize pipeline parallelism for efficient training in the presence of failures without spares. Bamboo [67] introduces redundant computation (RC) to provide resilience in the presence of frequent preemptions of training with spot instances. Oobleck [28] provides resiliency through creation of heterogeneous pipelines. SlipStream matches or outperforms them for a wide range of model sizes and failure frequencies.

## 7 Conclusion

SlipStream enables efficient DNN training in the presence of failures without the use of spare resources. SlipStream exploits the functional redundancies inherent to hybrid parallel training systems used for large DNNs. It introduces novel techniques to minimize the training throughput degradation of sustaining failures by exploiting unused resources (e.g., pipeline bubbles). We evaluated an end-to-end SlipStream prototype and showed it can tolerate a high numbers of concurrent failures for systems and models of various sizes. SlipStream improves training throughput under failures over Oobleck and Bamboo by up to 1.46× and 1.64× respectively.

## References

- [1] Josh others Achiam. 2023. GPT-4 Technical Report. *arXiv e-prints*, Article arXiv:2303.08774 (March 2023), arXiv:2303.08774 pages. <https://doi.org/10.48550/arXiv.2303.08774> arXiv:2303.08774 [cs.CL]
- [2] Meta AI. 2024. Meta Llama 3. <https://ai.meta.com/blog/meta-llama-3/>.
- [3] Sanjith Athlur, Nitika Saran, Muthian Sivathanu, Ramachandran Ramjee, and Nipun Kwatra. 2022. Varuna: scalable, low-cost training of massive deep learning models. In *Proceedings of the Seventeenth European Conference on Computer Systems (EuroSys '22)*. Association for Computing Machinery, New York, NY, USA, 472–487. <https://doi.org/10.1145/3492321.3519584>
- [4] David F. Bacon. 2022. Detection and Prevention of Silent Data Corruption in an Exabyte-scale Database System. In *The 18th IEEE Workshop on Silicon Errors in Logic – System Effects*.
- [5] Yixin Bao, Yanghua Peng, Chuan Wu, and Zongpeng Li. 2018. Online Job Scheduling in Distributed Machine Learning Clusters. arXiv:1801.00936 [cs.DC]
- [6] Romain Beaumont. 2022. Large Scale OpenCLIP: L/14, H/14 AND G/14 Trained on LAION-2B. <https://laion.ai/blog/large-openclip/>.
- [7] Stas Bekman. 2022. The Technology Behind BLOOM Training. <https://huggingface.co/blog/bloom-megatron-deepspeed>.
- [8] Rishi Bommasani et al. 2021. On the Opportunities and Risks of Foundation Models. *arXiv e-prints*, Article arXiv:2108.07258 (Aug. 2021), arXiv:2108.07258 pages. <https://doi.org/10.48550/arXiv.2108.07258> [cs.LG]
- [9] Tom B. Brown, Benjamin Mann, Nick Ryder, Melanie Subbiah, Jared Kaplan, Prafulla Dhariwal, Arvind Neelakantan, Pranav Shyam, Girish Sastry, Amanda Askell, Sandhini Agarwal, Ariel Herbert-Voss, Gretchen Krueger, Tom Henighan, Rewon Child, Aditya Ramesh, Daniel M. Ziegler, Jeffrey Wu, Clemens Winter, Christopher Hesse, Mark Chen, Eric Sigler, Mateusz Litwin, Scott Gray, Benjamin Chess, Jack Clark, Christopher Berner, Sam McCandlish, Alec Radford, Ilya Sutskever, and Dario Amodei. 2020. Language Models are Few-Shot Learners. *arXiv e-prints*, Article arXiv:2005.14165 (May 2020),

- arXiv:2005.14165 pages. <https://doi.org/10.48550/arXiv.2005.14165> arXiv:2005.14165 [cs.CL]
- [10] Zhenkun Cai, Xiao Yan, Kaihao Ma, Yidi Wu, Yuzhen Huang, James Cheng, Teng Su, and Fan Yu. 2022. TensorOpt: Exploring the Tradeoffs in Distributed DNN Training With Auto-Parallelism. *IEEE Transactions on Parallel and Distributed Systems* 33, 8 (Aug. 2022), 1967–1981. <https://doi.org/10.1109/tpds.2021.3132413>
- [11] Jianmin Chen, Xinghao Pan, Rajat Monga, Samy Bengio, and Rafal Jozefowicz. 2016. Revisiting Distributed Synchronous SGD. *arXiv e-prints*, Article arXiv:1604.00981 (April 2016), arXiv:1604.00981 pages. <https://doi.org/10.48550/arXiv.1604.00981> [cs.LG]
- [12] Trishul Chilimbi, Yutaka Suzue, Johnson Apacible, and Karthik Kalyanaraman. 2014. Project Adam: Building an Efficient and Scalable Deep Learning Training System. In *11th USENIX Symposium on Operating Systems Design and Implementation (OSDI 14)*. USENIX Association, Broomfield, CO, 571–582. <https://www.usenix.org/conference/osdi14/technical-sessions/presentation/chilimbi>
- [13] Databricks. 2024. Introducing DBRX: A New State-of-the-Art Open LLM. <https://www.databricks.com/blog/introducing-dbrx-new-state-art-open-llm/>.
- [14] Harish Dattatraya Dixit, Laura Boyle, Gautham Vunnam, Sneha Pendharkar, Matt Beadon, and Sriram Sankar. 2022. Detecting silent data corruptions in the wild. *arXiv e-prints*, Article arXiv:2203.08989 (March 2022), arXiv:2203.08989 pages. <https://doi.org/10.48550/arXiv.2203.08989> [cs.AR]
- [15] Jeffrey Dean, Greg Corrado, Rajat Monga, Kai Chen, Matthieu Devin, Mark Mao, Marc' aurelio Ranzato, Andrew Senior, Paul Tucker, Ke Yang, Quoc Le, and Andrew Ng. 2012. Large Scale Distributed Deep Networks. In *Advances in Neural Information Processing Systems*, F. Pereira, C.J. Burges, L. Bottou, and K.Q. Weinberger (Eds.), Vol. 25. Curran Associates, Inc. [https://proceedings.neurips.cc/paper\\_files/paper/2012/file/6aca97005c68f1206823815f66102863-Paper.pdf](https://proceedings.neurips.cc/paper_files/paper/2012/file/6aca97005c68f1206823815f66102863-Paper.pdf)
- [16] Jeffrey Dean and Sanjay Ghemawat. 2004. MapReduce: Simplified Data Processing on Large Clusters. In *6th Symposium on Operating Systems Design & Implementation (OSDI 04)*. USENIX Association, San Francisco, CA. <https://www.usenix.org/conference/osdi-04/mapreduce-simplified-data-processing-large-clusters>
- [17] DGX 2024. Nvidia DGX Systems. <https://www.nvidia.com/en-gb/data-center/dgx-systems/>.
- [18] Assaf Eisenman, Kiran Kumar Matam, Steven Ingram, Dheevatsa Mudigere, Raghuraman Krishnamoorthi, Krishnakumar Nair, Misha Smelyanskiy, and Murali Annaram. 2022. Check-N-Run: a Checkpointing System for Training Deep Learning Recommendation Models. In *19th USENIX Symposium on Networked Systems Design and Implementation (NSDI 22)*. USENIX Association, Renton, WA, 929–943. <https://www.usenix.org/conference/nsdi22/presentation/eisenman>
- [19] William Fedus, Barret Zoph, and Noam Shazeer. 2021. Switch Transformers: Scaling to Trillion Parameter Models with Simple and Efficient Sparsity. *arXiv e-prints*, Article arXiv:2101.03961 (Jan. 2021), arXiv:2101.03961 pages. <https://doi.org/10.48550/arXiv.2101.03961> [cs.LG]
- [20] Priya Goyal, Piotr Dollár, Ross Girshick, Pieter Noordhuis, Lukasz Wesolowski, Aapo Kyrola, Andrew Tulloch, Yangqing Jia, and Kaiming He. 2017. Accurate, Large Minibatch SGD: Training ImageNet in 1 Hour. *arXiv e-prints*, Article arXiv:1706.02677 (June 2017), arXiv:1706.02677 pages. <https://doi.org/10.48550/arXiv.1706.02677> [cs.CV]
- [21] Saurabh Gupta, Tirthak Patel, Christian Engelmann, and Devesh Tiwari. 2017. Failures in large scale systems: long-term measurement, analysis, and implications. In *Proceedings of the International Conference for High Performance Computing, Networking, Storage and Analysis (SC '17)*. Association for Computing Machinery, New York, NY, USA, Article 44, 12 pages. <https://doi.org/10.1145/3126908.3126937>
- [22] Gurobi 2024. <https://www.gurobi.com>.
- [23] Tao He, Xue Li, Zhibin Wang, Kun Qian, Jingbo Xu, Wenyuan Yu, and Jingren Zhou. 2023. Unicorn: Economizing Self-Healing LLM Training at Scale. *arXiv e-prints*, Article arXiv:2401.00134 (Dec. 2023), arXiv:2401.00134 pages. <https://doi.org/10.48550/arXiv.2401.00134> [cs.DC]
- [24] G. Hinton, L. Deng, D. Yu, G. E. Dahl, A. Mohamed, N. Jaitly, A. Senior, V. Vanhoucke, P. Nguyen, T. N. Sainath, and B. Kingsbury. 2012. Deep Neural Networks for Acoustic Modeling in Speech Recognition: The Shared Views of Four Research Groups. *IEEE Signal Processing Magazine* 29, 6 (2012), 82–97. <https://doi.org/10.1109/MSP.2012.2205597>
- [25] Jordan Hoffmann, Sebastian Borgeaud, Arthur Mensch, Elena Buchatskaya, Trevor Cai, Eliza Rutherford, Diego de Las Casas, Lisa Anne Hendricks, Johannes Welbl, Aidan Clark, Tom Hennigan, Eric Noland, Katie Millican, George van den Driessche, Bogdan Damoc, Aurelia Guy, Simon Osindero, Karen Simonyan, Erich Elsen, Jack W. Rae, Oriol Vinyals, and Laurent Sifre. 2022. Training Compute-Optimal Large Language Models. *arXiv e-prints*, Article arXiv:2203.15556 (March 2022), arXiv:2203.15556 pages. <https://doi.org/10.48550/arXiv.2203.15556> [cs.CL]
- [26] Yanping Huang, Youlong Cheng, Ankur Bapna, Orhan Firat, Mia Xu Chen, Dehao Chen, HyoukJoong Lee, Jiquan Ngiam, Quoc V. Le, Yonghui Wu, and Zhifeng Chen. 2019. *GPipe: efficient training of giant neural networks using pipeline parallelism*. Curran Associates Inc., Red Hook, NY, USA.
- [27] Changho Hwang, Taehyun Kim, Sunghyun Kim, Jinwoo Shin, and Kyoungsoo Park. 2021. Elastic Resource Sharing for Distributed Deep Learning. In *18th USENIX Symposium on Networked Systems Design and Implementation (NSDI 21)*. USENIX Association, 721–739. <https://www.usenix.org/conference/nsdi21/presentation/hwang>
- [28] Insu Jang, Zhenning Yang, Zhen Zhang, Xin Jin, and Mosharaf Chowdhury. 2023. Oobleck: Resilient Distributed Training of Large Models Using Pipeline Templates. In *Proceedings of the 29th Symposium on Operating Systems Principles (SOSP '23)*. Association for Computing Machinery, New York, NY, USA, 382–395. <https://doi.org/10.1145/360006.3613152>
- [29] Myeongjae Jeon, Shivaram Venkataraman, Amar Phanishayee, Junjie Qian, Wencong Xiao, and Fan Yang. 2019. Analysis of Large-Scale Multi-Tenant GPU Clusters for DNN Training Workloads. In *2019 USENIX Annual Technical Conference (USENIX ATC 19)*. USENIX Association, Renton, WA, 947–960. <https://www.usenix.org/conference/atc19/presentation/jeon>
- [30] Zhihao Jia, Matei Zaharia, and Alex Aiken. 2018. Beyond Data and Model Parallelism for Deep Neural Networks. arXiv:1807.05358 [cs.DC]
- [31] Yimin Jiang, Yibo Zhu, Chang Lan, Bairen Yi, Yong Cui, and Chuanxiong Guo. 2020. A Unified Architecture for Accelerating Distributed DNN Training in Heterogeneous GPU/CPU Clusters. In *14th USENIX Symposium on Operating Systems Design and Implementation (OSDI 20)*. USENIX Association, 463–479. <https://www.usenix.org/conference/osdi20/presentation/jiang>
- [32] Ziheng Jiang, Haibin Lin, Yinmin Zhong, Qi Huang, Yangru Chen, Zhi Zhang, Yanghua Peng, Xiang Li, Cong Xie, Shibiao Nong, Yulu Jia, Sun He, Hongmin Chen, Zhihao Bai, Qi Hou, Shipeng Yan, Ding Zhou, Yiyao Sheng, Zhuo Jiang, Haohan Xu, Haoran Wei, Zhang Zhang, Pengfei Nie, Leqi Zou, Sida Zhao, Liang Xiang, Zherui Liu, Zhe Li, Xiaoying Jia, Jianxi Ye, Xin Jin, and Xin Liu. 2024. MegaScale: Scaling Large Language Model Training to More Than 10,000 GPUs. In *21st USENIX Symposium on Networked Systems Design and Implementation (NSDI 24)*. USENIX Association, Santa Clara, CA, 745–760. <https://www.usenix.org/conference/nsdi24/presentation/jiang-ziheng>
- [33] Norman P. Jouppi, George Kurian, Sheng Li, Peter Ma, Rahul Nagarajan, Lifeng Nai, Nishant Patil, Suvinay Subramanian, Andy Swing, Brian Towles, Cliff Young, Xiang Zhou, Zongwei Zhou, and David Patterson. 2023. TPU v4: An Optically Reconfigurable Supercomputer

- for Machine Learning with Hardware Support for Embeddings. *arXiv e-prints*, Article arXiv:2304.01433 (April 2023), arXiv:2304.01433 pages. <https://doi.org/10.48550/arXiv.2304.01433> [cs.AR]
- [34] Jared Kaplan, Sam McCandlish, Tom Henighan, Tom B. Brown, Benjamin Chess, Rewon Child, Scott Gray, Alec Radford, Jeffrey Wu, and Dario Amodei. 2020. Scaling Laws for Neural Language Models. *arXiv e-prints*, Article arXiv:2001.08361 (Jan. 2020), arXiv:2001.08361 pages. <https://doi.org/10.48550/arXiv.2001.08361> [cs.LG]
- [35] Taebum Kim, Hyoungjoo Kim, Gyeong-In Yu, and Byung-Gon Chun. 2023. BPIPE: memory-balanced pipeline parallelism for training large language models. In *Proceedings of the 40th International Conference on Machine Learning (ICML 23)*. JMLR.org, Article 682, 15 pages.
- [36] Vijay Anand Korthikanti, Jared Casper, Sangkug Lym, Lawrence McAfee, Michael Andersch, Mohammad Shoeybi, and Bryan Catanzaro. 2023. Reducing activation recomputation in large transformer models. *Proceedings of Machine Learning and Systems 5* (2023).
- [37] Alex Krizhevsky. 2014. One weird trick for parallelizing convolutional neural networks. *arXiv e-prints*, Article arXiv:1404.5997 (April 2014), arXiv:1404.5997 pages. <https://doi.org/10.48550/arXiv.1404.5997> [cs.NE]
- [38] Alex Krizhevsky, Ilya Sutskever, and Geoffrey E. Hinton. 2017. ImageNet Classification with Deep Convolutional Neural Networks. *Commun. ACM* 60, 6 (May 2017), 84–90. <https://doi.org/10.1145/3065386>
- [39] Teven Le Scao et al. 2022. BLOOM: A 176B-Parameter Open-Access Multilingual Language Model. *arXiv e-prints*, Article arXiv:2211.05100 (Nov. 2022), arXiv:2211.05100 pages. <https://doi.org/10.48550/arXiv.2211.05100> [cs.CL]
- [40] Dmitry Lepikhin, Hyoungjoong Lee, Yuanzhong Xu, Dehao Chen, Orhan Firat, Yanping Huang, Maxim Krikun, Noam Shazeer, and Zhifeng Chen. 2020. GShard: Scaling Giant Models with Conditional Computation and Automatic Sharding. *arXiv e-prints*, Article arXiv:2006.16668 (June 2020), arXiv:2006.16668 pages. <https://doi.org/10.48550/arXiv.2006.16668> [cs.CL]
- [41] Mu Li, David G. Andersen, Jun Woo Park, Alexander J. Smola, Amr Ahmed, Vanja Josifovski, James Long, Eugene J. Shekita, and Bor-Yiing Su. 2014. Scaling Distributed Machine Learning with the Parameter Server. In *11th USENIX Symposium on Operating Systems Design and Implementation (OSDI 14)*. USENIX Association, Broomfield, CO, 583–598. [https://www.usenix.org/conference/osdi14/technical-sessions/presentation/li\\_mu](https://www.usenix.org/conference/osdi14/technical-sessions/presentation/li_mu)
- [42] Shigang Li and Torsten Hoefler. 2021. Chimera: efficiently training large-scale neural networks with bidirectional pipelines. In *Proceedings of the International Conference for High Performance Computing, Networking, Storage and Analysis (SC '21)*. Association for Computing Machinery, New York, NY, USA, Article 27, 14 pages. <https://doi.org/10.1145/3458817.3476145>
- [43] Shen Li, Yanli Zhao, Rohan Varma, Omkar Salpekar, Pieter Noordhuis, Teng Li, Adam Paszke, Jeff Smith, Brian Vaughan, Pritam Damania, and Soumith Chintala. 2020. PyTorch distributed: experiences on accelerating data parallel training. *Proc. VLDB Endow.* 13, 12 (aug 2020), 3005–3018. <https://doi.org/10.14778/3415478.3415530>
- [44] Haibin Lin, Hang Zhang, Yifei Ma, Tong He, Zhi Zhang, Sheng Zha, and Mu Li. 2019. Dynamic Mini-batch SGD for Elastic Distributed Training: Learning in the Limbo of Resources. *arXiv e-prints*, Article arXiv:1904.12043 (April 2019), arXiv:1904.12043 pages. <https://doi.org/10.48550/arXiv.1904.12043> [cs.LG]
- [45] Ziming Liu, Shenggan Cheng, Haotian Zhou, and Yang You. 2023. Hanayo: Harnessing Wave-like Pipeline Parallelism for Enhanced Large Model Training Efficiency. In *Proceedings of the International Conference for High Performance Computing, Networking, Storage and Analysis (SC '23)*. Association for Computing Machinery, New York, NY, USA, Article 56, 13 pages. <https://doi.org/10.1145/3581784.3607073>
- [46] Ilya Loshchilov and Frank Hutter. 2017. Decoupled Weight Decay Regularization. *arXiv e-prints*, Article arXiv:1711.05101 (Nov. 2017), arXiv:1711.05101 pages. <https://doi.org/10.48550/arXiv.1711.05101> [cs.LG]
- [47] Kshiteej Mahajan, Arjun Balasubramanian, Arjun Singhvi, Shivaram Venkataraman, Aditya Akella, Amar Phanishayee, and Shuchi Chawla. 2020. Themis: Fair and Efficient GPU Cluster Scheduling. In *17th USENIX Symposium on Networked Systems Design and Implementation (NSDI 20)*. USENIX Association, Santa Clara, CA, 289–304. <https://www.usenix.org/conference/nsdi20/presentation/mahajan>
- [48] Stephen Merity, Caiming Xiong, James Bradbury, and Richard Socher. 2016. Pointer Sentinel Mixture Models. arXiv:1609.07843 [cs.CL]
- [49] Jayashree Mohan, Amar Phanishayee, and Vijay Chidambaram. 2021. CheckFreq: Frequent, Fine-Grained DNN Checkpointing. In *19th USENIX Conference on File and Storage Technologies (FAST 21)*. USENIX Association, 203–216. <https://www.usenix.org/conference/fast21/presentation/mohan>
- [50] Deepak Narayanan, Aaron Harlap, Amar Phanishayee, Vivek Seshadri, Nikhil R. Devanur, Gregory R. Ganger, Phillip B. Gibbons, and Matei Zaharia. 2019. PipeDream: generalized pipeline parallelism for DNN training. In *Proceedings of the 27th ACM Symposium on Operating Systems Principles (SOSP '19)*. Association for Computing Machinery, New York, NY, USA, 1–15. <https://doi.org/10.1145/3341301.3359646>
- [51] Deepak Narayanan, Mohammad Shoeybi, Jared Casper, Patrick LeGresley, Mostofa Patwary, Vijay Korthikanti, Dmitri Vainbrand, Prithvi Kashinkunti, Julie Bernauer, Bryan Catanzaro, Amar Phanishayee, and Matei Zaharia. 2021. Efficient large-scale language model training on GPU clusters using megatron-LM. In *Proceedings of the International Conference for High Performance Computing, Networking, Storage and Analysis (SC '21)*. Association for Computing Machinery, New York, NY, USA, Article 58, 15 pages. <https://doi.org/10.1145/3458817.3476209>
- [52] Maxim Naumov, John Kim, Dheevatsa Mudigere, Srinivas Sridharan, Xiaodong Wang, Whitney Zhao, Serhat Yilmaz, Changkyu Kim, Hector Yuen, Mustafa Ozdal, Krishnakumar Nair, Isabel Gao, Bor-Yiing Su, Jiyang Yang, and Mikhail Smelyanskiy. 2020. Deep Learning Training in Facebook Data Centers: Design of Scale-up and Scale-out Systems. *arXiv e-prints*, Article arXiv:2003.09518 (March 2020), arXiv:2003.09518 pages. <https://doi.org/10.48550/arXiv.2003.09518> [cs.DC]
- [53] OpenAI. 2022. ChatGPT: Language models for task-oriented dialogue. <https://openai.com/blog/chatgpt/>.
- [54] Andrew Or, Haoyu Zhang, and Michael Freedman. 2020. Resource Elasticity in Distributed Deep Learning. In *Proceedings of Machine Learning and Systems*, I. Dhillon, D. Papailiopoulos, and V. Sze (Eds.), Vol. 2. 400–411. [https://proceedings.mlsys.org/paper\\_files/paper/2020/file/c443e9d9fc984cda1c5cc447e2c724d-Paper.pdf](https://proceedings.mlsys.org/paper_files/paper/2020/file/c443e9d9fc984cda1c5cc447e2c724d-Paper.pdf)
- [55] David A. Patterson, Garth Gibson, and Randy H. Katz. 1988. A case for redundant arrays of inexpensive disks (RAID). *SIGMOD Rec.* 17, 3 (jun 1988), 109–116. <https://doi.org/10.1145/971701.50214>
- [56] Yanghua Peng, Yixin Bao, Yangrui Chen, Chuan Wu, and Chuanxiong Guo. 2018. Optimus: an efficient dynamic resource scheduler for deep learning clusters. In *Proceedings of the Thirteenth EuroSys Conference (EuroSys '18)*. Association for Computing Machinery, New York, NY, USA, Article 3, 14 pages. <https://doi.org/10.1145/3190508.3190517>
- [57] PyTorch 2024. <https://pytorch.org/>.
- [58] Samyam Rajbhandari, Jeff Rasley, Olatunji Ruwase, and Yuxiong He. 2020. ZeRO: memory optimizations toward training trillion parameter models. In *Proceedings of the International Conference for High Performance Computing, Networking, Storage and Analysis (SC '20)*. IEEE Press, Article 20, 16 pages.
- [59] Samyam Rajbhandari, Olatunji Ruwase, Jeff Rasley, Shaden Smith, and Yuxiong He. 2021. ZeRO-infinity: breaking the GPU memory wall for extreme scale deep learning. In *Proceedings of the International Conference for High Performance Computing, Networking, Storage and Analysis (SC '21)*. Association for Computing Machinery, New York, NY, USA, Article 59, 14 pages. <https://doi.org/10.1145/3458817.3476205>



- [60] Jeff Rasley, Samyam Rajbhandari, Olatunji Ruwase, and Yuxiong He. 2020. DeepSpeed: System Optimizations Enable Training Deep Learning Models with Over 100 Billion Parameters. In *Proceedings of the 26th ACM SIGKDD International Conference on Knowledge Discovery & Data Mining (KDD '20)*. Association for Computing Machinery, New York, NY, USA, 3505–3506. <https://doi.org/10.1145/3394486.3406703>
- [61] Jie Ren, Samyam Rajbhandari, Reza Yazdani Aminabadi, Olatunji Ruwase, Shuangyan Yang, Minjia Zhang, Dong Li, and Yuxiong He. 2021. ZeRO-Offload: Democratizing Billion-Scale Model Training. In *2021 USENIX Annual Technical Conference (USENIX ATC 21)*. USENIX Association, 551–564. <https://www.usenix.org/conference/atc21/presentation/ren-jie>
- [62] Alexander Sergeev and Mike Del Balso. 2018. Horovod: fast and easy distributed deep learning in TensorFlow. *arXiv e-prints*, Article arXiv:1802.05799 (Feb. 2018), arXiv:1802.05799 pages. <https://doi.org/10.48550/arXiv.1802.05799> [cs.LG]
- [63] Noam Shazeer, Youlong Cheng, Niki Parmar, Dustin Tran, Ashish Vaswani, Penporn Koanantakool, Peter Hawkins, HyoukJoong Lee, Mingsheng Hong, Cliff Young, Ryan Sepassi, and Blake Hechtman. 2018. Mesh-TensorFlow: Deep Learning for Supercomputers. *arXiv e-prints*, Article arXiv:1811.02084 (Nov. 2018), arXiv:1811.02084 pages. <https://doi.org/10.48550/arXiv.1811.02084> [cs.LG]
- [64] Mohammad Shoeybi, Mostofa Patwary, Raul Puri, Patrick LeGresley, Jared Casper, and Bryan Catanzaro. 2019. Megatron-LM: Training Multi-Billion Parameter Language Models Using Model Parallelism. *CoRR* abs/1909.08053 (2019). arXiv:1909.08053 <http://arxiv.org/abs/1909.08053>
- [65] Shaden Smith, Mostofa Patwary, Brandon Norick, Patrick LeGresley, Samyam Rajbhandari, Jared Casper, Zhun Liu, Shrimai Prabhunoye, George Zerveas, Vijay Korthikanti, Elton Zhang, Rewon Child, Reza Yazdani Aminabadi, Julie Bernauer, Xia Song, Mohammad Shoeybi, Yuxiong He, Michael Houston, Saurabh Tiwary, and Bryan Catanzaro. 2022. Using DeepSpeed and Megatron to Train Megatron-Turing NLG 530B, A Large-Scale Generative Language Model. *arXiv e-prints*, Article arXiv:2201.11990 (Jan. 2022), arXiv:2201.11990 pages. <https://doi.org/10.48550/arXiv.2201.11990> [cs.CL]
- [66] Jakub M Tarnawski, Deepak Narayanan, and Amar Phanishayee. 2021. Piper: Multidimensional Planner for DNN Parallelization. In *Advances in Neural Information Processing Systems*, M. Ranzato, A. Beygelzimer, Y. Dauphin, P.S. Liang, and J. Wortman Vaughan (Eds.), Vol. 34. Curran Associates, Inc., 24829–24840. [https://proceedings.neurips.cc/paper\\_files/paper/2021/file/d01eeca8b24321cd2fe89dd85b9beb51-Paper.pdf](https://proceedings.neurips.cc/paper_files/paper/2021/file/d01eeca8b24321cd2fe89dd85b9beb51-Paper.pdf)
- [67] John Thorpe, Pengzhan Zhao, Jonathan Eyolfson, Yifan Qiao, Zhihao Jia, Minjia Zhang, Ravi Netravali, and Guoqing Harry Xu. 2023. Bamboo: Making Preemptible Instances Resilient for Affordable Training of Large DNNs. In *20th USENIX Symposium on Networked Systems Design and Implementation (NSDI 23)*. USENIX Association, Boston, MA, 497–513. <https://www.usenix.org/conference/nsdi23/presentation/thorpe>
- [68] Hugo Touvron et al. 2023. Llama 2: Open Foundation and Fine-Tuned Chat Models. *arXiv e-prints*, Article arXiv:2307.09288 (July 2023), arXiv:2307.09288 pages. <https://doi.org/10.48550/arXiv.2307.09288> [cs.CL]
- [69] Pablo Villalobos, Jaime Sevilla, Tamay Besiroglu, Lennart Heim, Anson Ho, and Marius Hobbhahn. 2022. Machine Learning Model Sizes and the Parameter Gap. *arXiv e-prints*, Article arXiv:2207.02852 (July 2022), arXiv:2207.02852 pages. <https://doi.org/10.48550/arXiv.2207.02852> [cs.LG]
- [70] Minjie Wang, Chien-chin Huang, and Jinyang Li. 2019. Supporting Very Large Models using Automatic Dataflow Graph Partitioning. In *Proceedings of the Fourteenth EuroSys Conference 2019 (EuroSys '19)*. Association for Computing Machinery, New York, NY, USA, Article 26, 17 pages. <https://doi.org/10.1145/3302424.3303953>
- [71] Stephanie Wang, John Liagouris, Robert Nishihara, Philipp Moritz, Ujval Misra, Alexey Tumanov, and Ion Stoica. 2019. Lineage stash: fault tolerance off the critical path. In *Proceedings of the 27th ACM Symposium on Operating Systems Principles (SOSP '19)*. Association for Computing Machinery, New York, NY, USA, 338–352. <https://doi.org/10.1145/3341301.3359653>
- [72] Tianyang Wang, Jun Huan, and Bo Li. 2018. Data Dropout: Optimizing Training Data for Convolutional Neural Networks. *arXiv e-prints*, Article arXiv:1809.00193 (Sept. 2018), arXiv:1809.00193 pages. <https://doi.org/10.48550/arXiv.1809.00193> [cs.CV]
- [73] Zhuang Wang, Zhen Jia, Shuai Zheng, Zhen Zhang, Xinwei Fu, T. S. Eugene Ng, and Yida Wang. 2023. GEMINI: Fast Failure Recovery in Distributed Training with In-Memory Checkpoints. In *Proceedings of the 29th Symposium on Operating Systems Principles (SOSP '23)*. Association for Computing Machinery, New York, NY, USA, 364–381. <https://doi.org/10.1145/3600006.3613145>
- [74] Qizhen Weng, Wencong Xiao, Yinghao Yu, Wei Wang, Cheng Wang, Jian He, Yong Li, Liping Zhang, Wei Lin, and Yu Ding. 2022. MLaaS in the Wild: Workload Analysis and Scheduling in Large-Scale Heterogeneous GPU Clusters. In *19th USENIX Symposium on Networked Systems Design and Implementation (NSDI 22)*. USENIX Association, Renton, WA, 945–960. <https://www.usenix.org/conference/nsdi22/presentation/weng>
- [75] Yang You, Zhao Zhang, Cho-Jui Hsieh, James Demmel, and Kurt Keutzer. 2017. ImageNet Training in Minutes. *arXiv e-prints*, Article arXiv:1709.05011 (Sept. 2017), arXiv:1709.05011 pages. <https://doi.org/10.48550/arXiv.1709.05011> [cs.CV]
- [76] Susan Zhang, Stephen Roller, Naman Goyal, Mikel Artetxe, Moya Chen, Shuohui Chen, Christopher Dewan, Mona Diab, Xian Li, Xi Victoria Lin, Todor Mihaylov, Myle Ott, Sam Shleifer, Kurt Shuster, Daniel Simig, Punit Singh Koura, Anjali Sridhar, Tianlu Wang, and Luke Zettlemoyer. 2022. OPT: Open Pre-trained Transformer Language Models. *arXiv e-prints*, Article arXiv:2205.01068 (May 2022), arXiv:2205.01068 pages. <https://doi.org/10.48550/arXiv.2205.01068> [cs.CL]
- [77] Yanli Zhao, Andrew Gu, Rohan Varma, Liang Luo, Chien-Chin Huang, Min Xu, Less Wright, Hamid Shojanazeri, Myle Ott, Sam Shleifer, Alban Desmaison, Can Balioglu, Pritam Damania, Bernard Nguyen, Geeta Chauhan, Yuchen Hao, Ajit Mathews, and Shen Li. 2023. PyTorch FSDP: Experiences on Scaling Fully Sharded Data Parallel. *arXiv e-prints*, Article arXiv:2304.11277 (April 2023), arXiv:2304.11277 pages. <https://doi.org/10.48550/arXiv.2304.11277> [cs.DC]
- [78] Lianmin Zheng, Zhuohan Li, Hao Zhang, Yonghao Zhuang, Zhifeng Chen, Yanping Huang, Yida Wang, Yuanzhong Xu, Danyang Zhuo, Eric P. Xing, Joseph E. Gonzalez, and Ion Stoica. 2022. Alpa: Automating Inter- and Intra-Operator Parallelism for Distributed Deep Learning. In *16th USENIX Symposium on Operating Systems Design and Implementation (OSDI 22)*. USENIX Association, Carlsbad, CA, 559–578. <https://www.usenix.org/conference/osdi22/presentation/zheng-lianmin>
- [79] Yazhou Zu, Alireza Ghaffarkhah, Hoang-Vu Dang, Brian Towles, Steven Hand, Safeen Huda, Adekunle Bello, Alexander Kolbasov, Arash Rezaei, Dayou Du, Steve Lacy, Hang Wang, Aaron Wisner, Chris Lewis, and Henri Bahini. 2024. Resiliency at Scale: Managing Google’s TPUv4 Machine Learning Supercomputer. In *21st USENIX Symposium on Networked Systems Design and Implementation (NSDI 24)*. USENIX Association, Santa Clara, CA, 761–774. <https://www.usenix.org/conference/nsdi24/presentation/zu>